Nuclear Bond Models of Stellar Nucleosynthesis

Peter Norman, Monash University, Retired

Contents **Page**

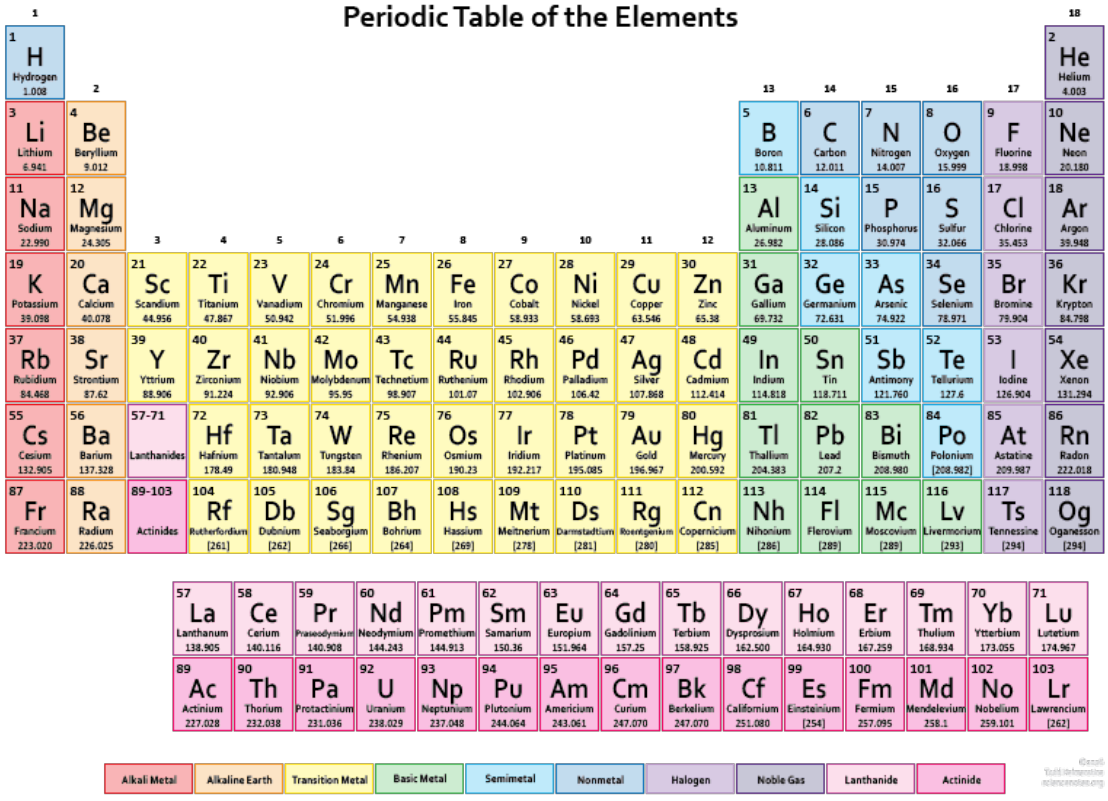

In this document each nucleus will be symbolised as shown below for helium:

$^{4}He_{2}$ where 2 = number of protons = atomic number = Z
and 4 = number of protons + neutrons = mass number = A

Preface

Recently cosmologists decided that the universe began nearly 14 billion years ago from nothing as a hot, dense mass of plasma that rapidly expanded and cooled to form stars. I have been guided in writing this account by the details of much recent nuclear research published in the book entitled " Cauldrons in the Cosmos ". The authors, Rolfs and Rodney (1988), of this modern Dreamtime story have outlined the details of the probable nuclear evolution of all the elements that I have modelled

No discussion is made here of the subsequent fascinating evolution of countless mixtures and compounds of atoms of elements that have slowly evolved from the elements during the last 5 billion years since the solar system began. These recent chemical changes have occurred at much lower temperatures and involved energies a million times less than in nuclear reactions!

This story began during the 1960s when I was a young chemistry teacher in the process of constructing scale models of simple molecules. Because these models were very good teaching aids I planned to make similar models of common nuclei. The stimulus for this desire was the recent realisation by astro-physicists that most nuclei are synthesised in the hot cores of massive stars. Unfortunately a quick review of my third year university physics texts showed that such simple models did not exist! So began my quest. I first calculated the num ber of bonds in each light nucleus and then made simple ball and stick models by joining small hollow plastic balls with short wood dowels, one dowel for each nuclear bond. I had punctured each ball with 12 equally spaced holes to facilitate appropriate bonding on the assumption that 12:12 coordination is the maximum for spheres. I was pleased to find how consistently elegant the models were - but they became cumbersome as the number of dowels increased. I then used table-tennis balls for nucleons joined by a drop of glue, from a glue gun, one drop for each bond.

By this time I realised the importance of the underlying alpha structure of hevier nuclei and started modelling with one table-tennis ball for each alpha.

Photos of two early models of ^{56}Ni.
The model on the left shows the average arrangement of the 126 bonds between the 56 nucleons. In the centre, the model indicates close packing of the 56 nucleons. On the right is a recent model of ^{56}Ni seen as 14 close packed alphas

Table of Terms and Symbols

alpha = α = alpha particle = $^{4}He_{2}$

anti-particle of X = X with opposite electric charge. eg. e^{+} and e^{-}

atom = smallest form of an element

atomic number = Z = number of protons in a nucleus

beta = β = beta particle = β^{+} or β^{-}

delta = Δ = defect or difference or change, eg: Δm and ΔE

deuteron = $^{2}H_{1}$ = nucleus of deuterium

electron = e^{-} = β^{-} = point-like elementary particle with mass = 1/1800 of proton mass

electron volt = 1 (eV) = unit of energy

fermi = 1 (fm) = 10^{-15}(m) = diameter of a nucleon

gamma = γ = gamma ray = high energy photon

isotopes of an element have the same proton number, Z, but different neutron numbers = A-Z

mass number = A = number of protons + neutrons in a nucleus

mass-energy equation = $E = mc^{2}$ or $\Delta E = \Delta mc^{2}$

mass defect = Δm = mass difference between a nucleus and mass of its nucleons

neutron = n^{0} = a nucleon = elementary particle with mass slightly heavier than a proton

neutrino = ν = very small particle witth very low mass

nuclear fission = splitting a nucleus into 2 or more nuclei

nuclear fusion = combining 2 or more nuclei into a nucleus

nucleo-synthesis = synthesis of a nucleus by nuclear fusion

nucleus = small heavy core of an atom defined by A and Z

positron = positive electron = $e^{+} = \beta^{+}$

proton = p^{+} = $^{1}H_{1}$ = a nucleon = elementary particle with mass = 18 00 electrons

speed of light = c = 300,000 km/sec.

triton = $^{3}H_{1}$ = nucleus of tritium

Chapter 1. The Nuclear Atom

1.1 Elements and Atoms

Over 2000 years ago several Greek and Roman scholars suggested that all matter consists of mixtures and compounds of very small and unique atoms of a finite number of elements. Unfortunately, Aristotle decided there were only 4 : earth, water, air and fire. These ideas were useless until 200 years ago when Dalton, an English chemist, adopted and extended them to accommodate recently discovered properties of elements. In particular Dalton showed that the chemical rules of constant and multiple proportions of the weights of different elements in compounds were consistent with the idea of the unique atomic masses of the elements involved.

Subsequent experiments with measured volumes of gases by other chemists improved Dalton's atomic theory.

1.2 The electrical properties of matter

Late in the 1700s the French physicist ,Coulomb showed that bodies could be given either a positive or a negative charge. Furthermore he found that when two bodies were both charged either positively or negatively then the two like charges repelled each other with a force proportional to the product of the two charges and inversely as the square of their separation. He also found that the same rule was true for the attraction between two unlike charges.

About 50 years later the Scottish physicist Maxwell suggested that electric charge existed as very small positive or negative "atoms" of electricity..

By 1890 an English physicist, Thomson was able to measure the charge/mass ratio of the smallest "atom" of negative electricity called an electron was 1/1.. In 1906 Thomson also found the charge/mass ratio of the positive proton was1/1800.

1.3 The "Plum Pudding" atom

On the basis of these measurements Thomson therefore thought of a hydrogen atom as a single "pudding" proton 1800 times larger than a single "plum" electron in the middle of the pudding. Atoms of heavier elements would consist of a larger pudding with the relevant number of embedded plums. Unfortunately at that time there was no available way of testing this model of the atom.

1.4 The Nuclear Atom

Then in 1896 the French physicist Becquerel accidentally discovered the radioactivity of uranium. The New Zealand physicist Rutherford soon found that the radiation consisted of alpha, beta and gamma rays. In his study of alpha rays by shooting a stream of them at a thin film of gold foil he found that most of them passed straight through the gold atoms! Because only a few alphas actually bounced back from the foil Rutherford rejected the plum pudding model of the atom and decided that the more massive protons formed a central nucleus surrounded by an equal number of less massive electrons occupying a much larger volume. He illustrated this by saying that if an atom was the size of a large room the nucleus would only be as big as a small grain of sand! However it was soon found that most nuclei are more massive than the relevant number of protons.

The problem was solved in 1932 when the English physicist Chadwick discovered the neutral neutron with a mass similar to that of the proton. For this reason the helium nucleus or alpha particle was described as 2 protons and 2 neutrons tightly bound together.
This discovery quickly led to the series of attempts to account for the underlying structure of nuclei in terms of alpha particles

Chapter 2. Early models of nuclear bonds and structures

2.1 Alpha particle models

The American nuclear chemist Harkins noted that nuclei whose mass numbers are multiples of 4 have more stability than other nuclei. He also noted that the most plentiful nuclei in stars, meteorites and on the earth could be considered as clusters of alpha particles. Rutherford subsequently confirmed these observations by showing that such abundant nuclei were more stable to alpha particle bombardment.

Furthermore, Harkins noted that the atomic weight of helium is slightly less than the sum of the atomic weights of four hydrogen atoms. This difference, the mass defect, he correctly explained in terms of Einstein's equivalence of mass and energy as the amount of energy that would be released if four hydrogen nuclei fused to form a helium nucleus. This prediction, made in 1915, was endorsed four years later by Perrin.

In 1920 Harkins also predicted the existence of the neutron and heavy hydrogen. As a result of his experiments with his cyclotron in the 1930s he suggested that the source of the sun's energy was probably the fusion of hydrogen into helium.

When Chadwick first identified the neutron in 1932 the concept of the alpha **particle** was simplified so that quite a few nuclear physicists attempted to develop better alpha particle models of nuclei. Some of these physicists were Wheeler and Farno in 1937, Weizsacker, Hafstead and Teller in 1938.

Their models were rejected because they assumed that the nuclear bond energy only consisted of the binding energy as measured by the mass defect. Another reason was due to the geometry of their models.

2.2 Liquid drop models

In 1929 Gamow presented a paper at the Royal Society proposing a simple model of a nucleus built from alpha particles in a way very similar to a water drop held together by surface tension. In this way he attempted to model the mass-defect curve of nuclear structure. In 1935 Weizsacker described the nucleus as a semi-classical fluid of protons and neutrons with an internal repulsive Coulomb force between the protons. The quantum mechanical nature of these nucleons was made via the Pauli exclusion principle. This effectively modelled the nucleus as a Fermi liquid.

Bohr, in 1936 also adopted the liquid drop model of nuclear structure which both he and Gamow used to describe nuclear fission in 1939.

2.3 Shell models

As proposed in 1932 the first nuclear shell model was an analogue of the energetically successful atomic model of closed shells of electrons. As such the nuclear shell model was an improvement on the liquid drop model. In 1949 this model was extended by Wigner, Mayer and Jensen who invoked the Pauli principle and spin orbit coupling to account for the stability of "magic numbers" of nucleons, namely: 2, 8, 20, 28, 50, 82 or 126.

Chapter 3. Solar nucleo-synthesis of helium

3.1 Synthesis of a deuteron

As it has been established that helium nuclei are synthesised from hydrogen in the hot core of the sun and all other stars of the same mass, it will be convenient to first model this process. It begins when a neutron collides with a proton with enough energy to bind them together, as a deuteron, by a strong nuclear bond . In this case the nuclear bond energy, En is equal to the nuclear binding energy, Eb. This energy is released as a gamma ray and is equal to the mass defect between the mass of the deuteron formed and the larger sum of the masses of the free proton and neutron. According to Einstein's rule, $E = mc^2$ where E is the energy released, m is the mass defect and c is the speed of light = 300,000 km per sec. The standard unit of nuclear energy is one million electron volts = 1 (MeV).

The modelling of this fusion is shown in Table 3.1 and Fig.3.1.

Nucleus	**^{1}H +**	**n →**	**^{2}H**	**Energy change**
Energy	**A**	**B**	**C**	**ΔE = C - A - B**
Eb (MeV)	-	-	2.2	**ΔEb = 2.2 (MeV)**
= En (MeV)	-	-	2.2	**=ΔEn = 2.2 (MeV)**

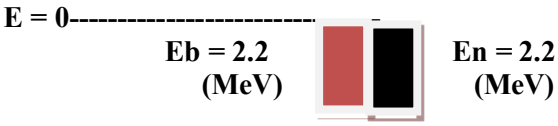

Table 3 Changes in nuclear bond energy data during the nucleosynthesis of ^{2}H.

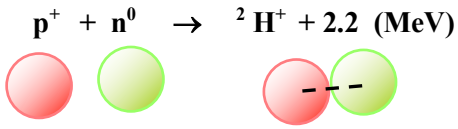

Figure 3.1. Models of the ^{1}H and ^{2}H nuclei and their energy data.

It is significant in this fusion that for ^{2}H, En equals Eb because no repulsive Coulomb energy is involved.

3.2 Synthesis of a triton

The changes during the fusion of a neutron with a deuteron are shown in Table 3.2 and Fig.3.2 .

Nucleus	**^{2}H +**	**n →**	**^{3}H**	**Energy change**
Energy	**A**	**B**	**C**	**ΔE = C - A - B**
Eb (MeV)	2.2	-	8.5	**ΔEb = 6.3 (MeV)**
= En (MeV)	2.2	-	8.5	**=ΔEn = 6.3 (MeV)**

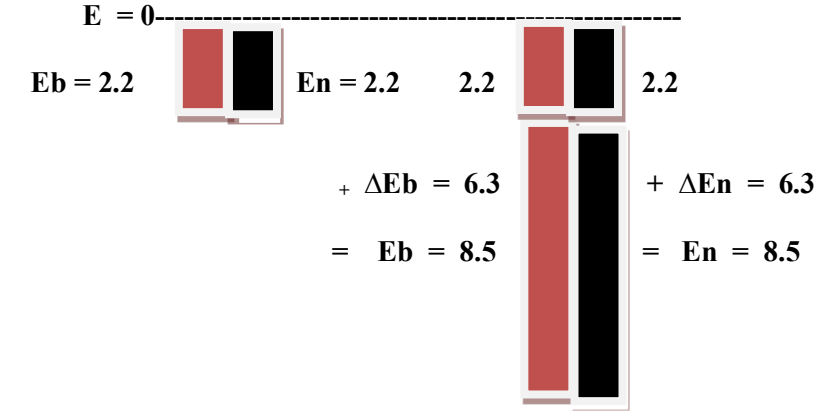

Table 3.2 Changes in nuclear bond energy data during the synthesis of ^{3}H.

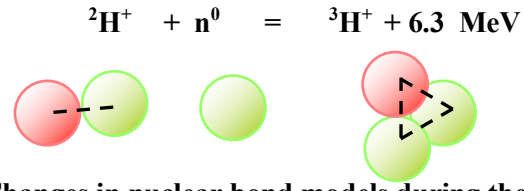

Figure 3.2 Changes in nuclear bond models during the synthesis of ^3H.

The model of triton is triangular so that each nucleon is close enough to each of the other two nucleons to be strongly bound to it by a nuclear bond. Only in this way is the nucleus most stable , that is, in its ground state. Bernal [1960] used similar methods when modelling a liquid drop of an element or compound with different numbers of atoms or molecules. He described this close packing as placing the next atom (or molecule) as close as possible to the centre of the drop.

3.3 Synthesis of a helium 3 nucleus

By contrast with the previous two fusions, considerably more energy is required to fuse a proton with a deuteron to form a helium 3 nucleus. This is because of the strong Coulomb repulsion between the two protons in $^3He^{++}$. However, when the colliding proton is close enough to the deuteron to trigger bonding, the nuclear bond energy, En is equal to the attractive energy required to just balance the repulsive Coulomb energy, Ec, plus the binding energy released, Eb. The data and models of this fusion are shown in Table 3.3 and Fig. 3.3.

Nucleus	**$^2H^+$ +**	**$p^+ \rightarrow$**	**$^3He^{++}$**	**Energy change**
Energy	A	B	C	**ΔE = C - A - B**
Eb (MeV)	2.2	-	7.7	**ΔEb = 5.5 (MeV)**
+ Ec (MeV)	-	-	0.9	**+ΔEc = 0.9 (MeV)**
= En (MeV)	2.2	-	8.6	**=ΔEn = 6.4 (MeV)**

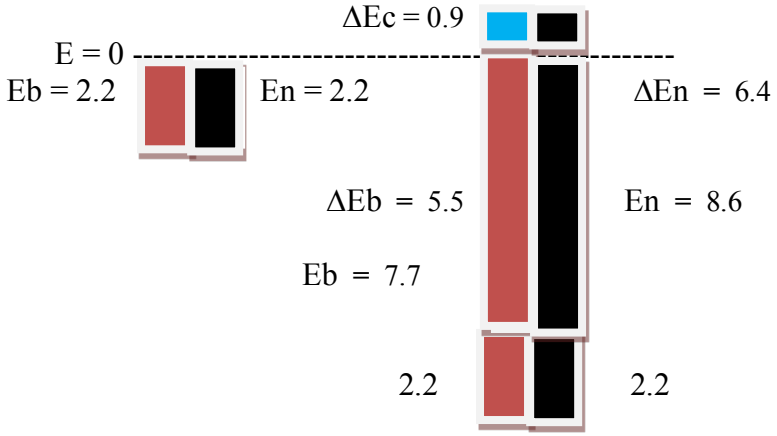

Table 3.3 Changes in nuclear bond energy data during the synthesis of ^3He.

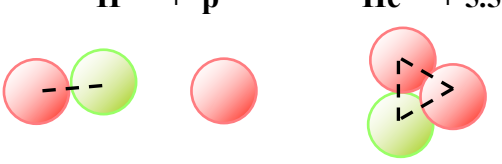

Figure 3.3 Changes in nuclear bond m odels during the synthesis of ^3He.

It is interesting to note that En = 8.6(MeV) for ^{3}He which is very close to En = 8.5 (MeV) for ^{3}H. That is, the nuclear bond energy between the three nucleons in ^{3}He makes it more stable than ^{3}H. It is for this reason that ^{3}H undergoes b eta$^-$ decay to form more stable ^{3}He as shown below.

Nucleus	**$^3H^+ \rightarrow$**	**e^- +**	**$^3He^{++}$**	**Energy change**
Energy	**A**	**B**	**C**	**ΔE = B +C- A**
Eb (MeV)	8.5	-	7.7	**ΔEb = - 0.8**(MeV)
+ Ec (MeV)	-	-	0.9	**+ ΔEc = 0.9 (MeV)**
= En (MeV)	8.5	-	8.6	**=ΔEn = 0.1 (MeV)**

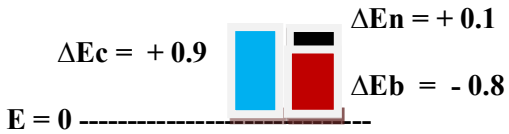

Table 3.4 Changes in nuclear bond energy data during the beta$^-$ decay of ^{3}H.

This demonstrates that. the repulsive Coulomb energy between the two protons arises as the electron escapes. This energy not only creates the slight increase in bond energy but also makes the ^{3}He more massive than the ^{3}H. This decay is a fission reaction.

3.4 The repulsive Coulomb energy of a nucleus

Coulomb energy of a nucleus containing more than one proton is calculated by a simple formula derived in the following way from Coulomb's law.

$$E_c = \frac{3\,Z(Z-1)\,e^2}{5\,r_o\,A^{1/3}} = \frac{a\,Z(Z-1)}{A^{1/3}} \quad \text{where} \quad e^2 = 1.44\ (\text{MeV. fm}) \quad \text{and} \quad r_o = 1.15\ (\text{fm})$$

$$\text{so} \quad a = \frac{3\,e^2}{5\,r_o} = \frac{3 \times 1.44}{5 \times 1.15} = 0.67\ (\text{MeV})$$

$$\text{so} \quad \mathbf{E_c = \frac{0.67\ Z(Z-1)}{A^{1/3}}}$$

3.5 Nuclear energies and their changes

The term nuclear energy as used in this simple account will be restricted to those involved with inter-nucleon bonding namely- binding energy Eb, Coulomb energy Ec and nuclear bond energy En. These energies are related by the identity: En = Eb + Ec .

In each of the nuclear reactions above the energy changes satisfy the following identity:

ΔEn = ΔEb + ΔEc or ΔEb = ΔEn - ΔEc or ΔEc = ΔEn - ΔEb

Essentially the type of change that occurs depends on the relative size of ΔEn and ΔEc. Fusion occurs when the attractive energy change, ΔEn is larger than the repulsive change, ΔEc. Fusions release free energy, ΔEb, as a combination of kinetic and radiant energy as frozen mass energy of the reactants is reduced.

By contrast, when decay or fission occurs, ΔEc is larger than ΔEn so that in alpha decay, beta$^+$ decay, beta$^-$ decay and fission, binding energy is released as repulsive Coulomb energy prevails over attractive nuclear bond energy.

The origin of En, Ec and Eb as well as charge and mass is within each nucleon and its quarks and gluons. However, this simple account is only concerned with inter-nucleon activity and not with intra-nucleon behaviour.

3.6 Synthesis of a helium 4 nucleus

When two ^{3}He nuclei fuse together in the core of the sun they form a nucleus of ^{4}He and two free protons. This fusion is the last step in the first stage of forming ^{4}He in the sun. This stage, known as P-P I, is shown below.

P-P I: (31%) $^{1}H + {}^{2}H \rightarrow 3He$; $^{3}He + {}^{3}He \rightarrow {}^{4}He + 2.{}^{1}H$

The changes during the fusion of two ^{3}He nuclei are shown in Table 3.5 and Fig. 3.4.

Nucleus	2. ^{3}He →	2. ^{1}H +	^{4}He	**Energy change**
Energy	**A**	**B**	**C**	**ΔE = B + C - A**
Eb (MeV)	15.4	-	28.3	**ΔEb = 12.9 (MeV)**
+ Ec (MeV)	1.8	-	0.8	**+ ΔEc = - 1.0 (MeV)**
= En (MeV)	17.2	-	29.1	**= ΔEn = 11.9 (MeV)**

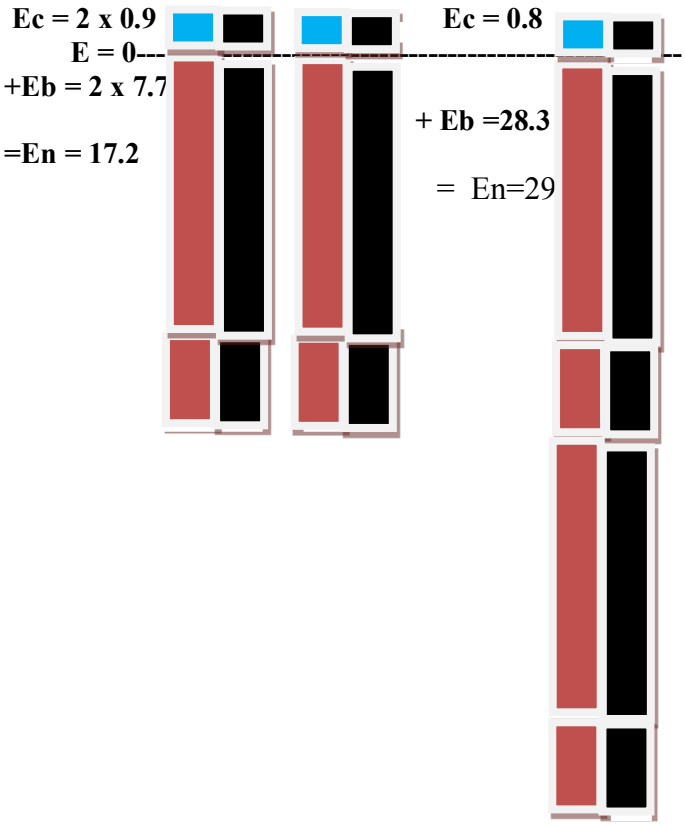

Table 3.5 Energy data of fusion of two ^{3}He nuclei.

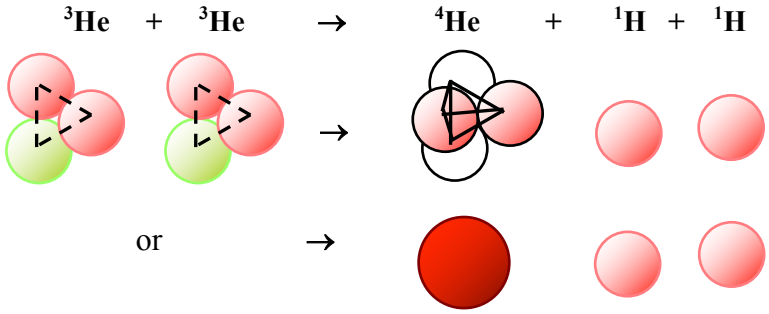

Figure 3.4 Changes in nuclear bond models during the synthesis of ^{4}He**.**

3.7 Definition of a unit nuclear bond

The model of the alpha in Fig. 3.4 shows 3 nuclear bonds between each of the 4 nucleons via 3 of the 12 points of close contact of each nucleon. It is assumed that the strong, attractive nuclear bonds act equally between all nucleons by some mutual exchange mechanism. Furthermore, because the spin of each member of the pair of protons and neutrons is the reverse of the other member, it is assumed that each alpha is a boson. Also, because the Eb per nucleon of an alpha is so large, it is proposed that a convenient unit nuclear bond energy, En will be arbitrarily defined as follows:

$$\textbf{One nuclear bond} = 1\ (\text{NB}) = \frac{\text{En of } {}^4\text{He}}{6} = \frac{29.1}{6}\ (\text{MeV}) = 4.84\ (\text{MeV})$$

Henceforth this unit will be used to simplify the ensuing modelling of heavier nuclei. Furthermore, because of the unique properties of ^{4}He, it is proposed to mainly model nuclei that may be composed mostly of integral multiples of alphas. In this respect the models will conform with those proposed by Ikeda [1967], Horiuchi [1972] and Norman [2003]. In their models of excited nuclei it was assumed that the nuclear bond energy of each alpha did not change whereas the nuclear bonds between alphas were either weakened or broken by extra excitation energy.

3.8 More solar syntheses of a helium 4 nucleus

The sun produces its helium 4 and radiant energy by the processes P-P I, II and III.

P-P II: (68.8%) $^1\text{H} + {}^2\text{H} \rightarrow {}^3\text{He}$; $^3\text{He} + {}^4\text{He} \rightarrow {}^7\text{Be}$;

$^7\text{Be} + \beta^- \rightarrow {}^7\text{Li} + \nu$; $^7\text{Li} + {}^1\text{H} \rightarrow {}^8\text{Be}$; $^8\text{Be} \rightarrow 2.{}^4\text{He}$

P-P III: (0.2%) $^1\text{H} + {}^2\text{H} \rightarrow {}^3\text{He}$; $^3\text{He} + {}^4\text{He} \rightarrow {}^7\text{Be}$;

These reactions effectively convert 616 million tons of hydrogen into helium every second. Details of the synthesis of ^{7}Be are shown below.

Nucleus	**^{3}He +**	**^{4}He →**	**^{7}Be**	**Energy change**
Energy	**A**	**B**	C	ΔE = **C - A- B**
Eb (MeV)	7.7	28.3	37.6	ΔEb = **1.6 (MeV)**
+ Ec (MeV)	0.9	0.8	4.2	+ ΔEc = **2.5 (MeV)**
= En (MeV)	8.6	29.1	41.8	= ΔEn = 4.1 **(MeV)**
= En (NB)	1.8=(3x0.6)	6=(6x1)	8.6=(6+3x0.6 + 0.8)	= **ΔEn = *0.8 (NB)***

Table 3.6 Changes in nuclear bond energy data during the synthesis of ^{7}Be.

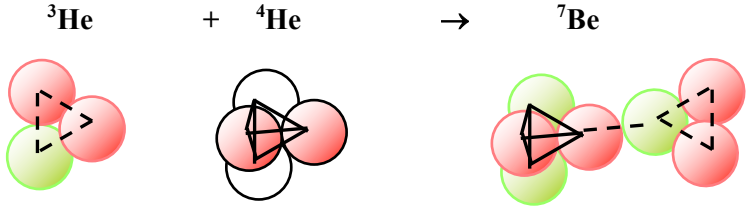

Figure 3.5 Changes in nuclear bond models during the synthesis of ^{7}Be.

Nucleus	**^{7}Be →**	**e^+**	**+ ^{7}Li**	**Energy change**
Energy	A	**B**	C	**ΔE = B+ C - A**
Eb (MeV)	37.6	-	39.3	**ΔEb = 1.7 (MeV)**
+ Ec(MeV)	4.2	-	2.1	**+ ΔEc = - 2.1 (MeV)**
= En (MeV)	41.8	-	41.4	**= ΔEn = - 0.4 (MeV)**
= En (NB)	8.6=(6+3x0.6 + 0.8)	-	8.5=(6+4x0.6)	**= ΔEn = - 0.1 (NB)**

Table 3.7 Changes in nuclear bond energy data during beta$^+$ decay of ^{7}Be.

This beta decay occurs because ΔEc decrease is larger than ΔEn decrease . That is, the emission of a positron (positive electron) reduces the Coulomb repulsion so the nuclear bond energy relaxes as free binding energy escapes as mass reduces.
ie. repulsion is dominant.

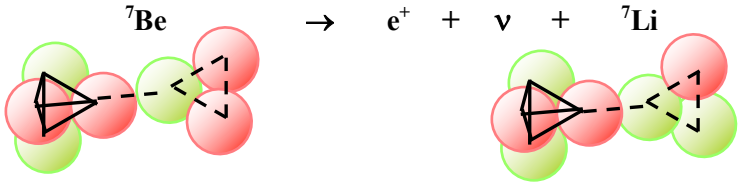

Figure 3.6 Changes in nuclear bond energy models during the beta decay of ^{7}Be.

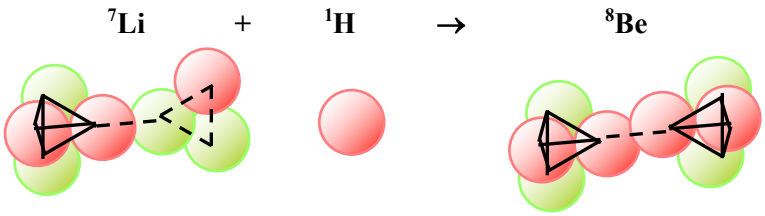

Figure 3.7 Changes in nuclear bond energy models during the origin of ^{8}Be.

The changes during the fission of ^{8}Be into two alphas are shown in Table 3.8 and Fig.3.8.

Nucleus	^{8}Be →	^{4}He +	^{4}He	Energy change
Energy	A	B	C	ΔE = B + C - A
Eb (MeV)	56.5	28.3	28.3	ΔEb = 0.1 (MeV)
+ Ec (MeV)	4.0	0.8	0.8	+ ΔEc = -2.4 (MeV)
= En (MeV)	60.5	29.1	29.1	= ΔEn = - 2.3 (MeV)
= En (NB)	12.4=.(2x6+0.4)	6= (6x1)	6= (6x1)	= ΔEn = - 0.*4* (NB)

Table 3.8 Changes in nuclear bond energy data during the fission of ^{8}Be.

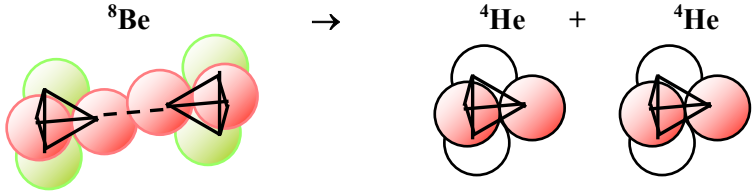

Figure 3.8 Changes in nuclear bond models during the fission of ^{8}Be.

This alpha decay occurs as 0.4 (NB) breaks because ΔEc is larger than ΔEn.
The half -life of very unstable ^{8}Be is only 10^{-16} sec.

Chapter 4. Synthesis of carbon, nitrogen and oxygen in red giant stars

4.1 Hoyle's problem

During the 1940s Gamow argued that all elements would have been created in the hot Big Bang. Hoyle claimed that the early universe could only make hydrogen and some helium. So Gamow joked: *In the beginning God said, "Let there be Hoyle." And there was Hoyle. And God looked at Hoyle and told him to make heavy elements in any way he pleased. And Hoyle decided to make heavy elements in stars and to spread them around by supernovae explosions!*

However, Hoyle soon came upon a problem. In giant stars 1.5 times heavier than the sun their core temperatures are around 100 million K. At these temperatures the ^{4}He nuclei first formed in the stellar cores collide with each other to form ^{12}C nuclei in the simple manner first proposed by Hoyle .

According to Fowler Hoyle's problem in 1952 was that nucleosynthesis in stars could not proceed beyond the formation of ^{4}He nuclei. This is because the ^{8}Be nucleus formed by the fusion of two ^{4}He nuclei is so unstable that it has a half life of only 10^{-16} seconds as it decays back into helium in the reversible reaction:

2.^{4}He $\leftrightarrow$ ^{8}Be. This means that at 10^{8} K in the core of a red giant star there is only one ^{8}Be nucleus per billion ^{4}He nuclei. Therefore very few stable ^{12}C nuclei in their ground state can be formed by the direct fusion of a ^{4}He nucleus with a ^{8}Be nucleus in the reaction: ^{4}He + ^{8}Be $\rightarrow$ ^{12}C

Hoyle reasoned that for this rate to be increased the fusion reaction must be 'resonant'. That is, the ^{12}C nuclei must initially be formed in an excited state, ^{12}C*, such that the net binding energy, Eb, of each ^{12}C* nucleus would be less than the sum of the net binding energies of the ^{4}He and ^{8}Be nuclei by an amount equal to Er = 0.3 MeV. This value of Er is that of the most energetic nuclei in stellar cores at 10^{8} K. Hoyle believed that the very existence of living things based on carbon, depends on the existence of such an excited state in carbon but it had never previously been known to exist. Significantly, carbon is the fourth most abundant element in the universe. As a result of more experiments Hoyle's prediction of the excitation energy of carbon was confirmed at 7.68 (MeV) .

The details of the successful triple alpha fusion are shown below.

Nucleus	**^{8}Be +**	**^{4}He $\rightarrow$**	**^{12}C***	**Energy change**
Energy	A	B	**C**	**ΔE = C - A- B**
Eb (MeV)	56.5	28.3	84.4	**ΔEb= -0.4 (MeV) = Er !**
+ Ec (MeV)	4.0	0.8	7.2	**+ ΔEc = 2.4 (MeV)**
= En (MeV)	60.5	29.1	91.6	**= ΔEn = 2.0 (MeV)**
= En (NB)	12.4=.(2x6+0.4)	6= (1x6)	19=(3x6)+1	**= ΔEn = 0.5 (NB)**

Table 4.1 Changes in nuclear bond energy data during the fusion of ^{12}C* .
^{8}Be + ^{4}He $\rightarrow$ ^{12}C*

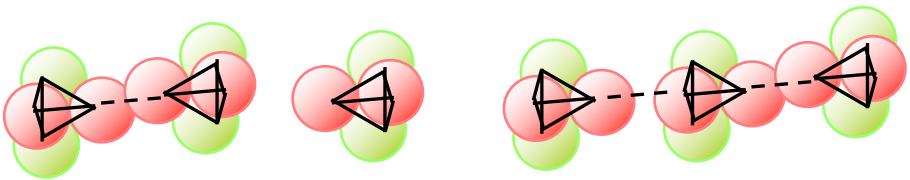

Figure 4.1 Changes in nuclear bond m odels during the fusion of ^{12}C*.
The details of the subsequent gamma ray emission of excitation energy as ^{12}C* decays to ^{12}C are shown below.

Nucleus	$^{12}C^*$ →	^{12}C	Energy change
Energy	**A**	**B**	**ΔE = B - A**
Eb (MeV)	84.4	92.1	**ΔEb = 7.7 (MeV)**
+ Ec (MeV)	7.2	8.8	**ΔEc = 1.6 (MeV)**
= En (MeV)	91.6	100.9	**ΔEn = 9.3 (MeV)**
= En (NB)	19=(3x6)+(2x0.5)	20.8=(3x6)+ (3x0.9)	**ΔEn = 1.8 (NB)**

Table 4.2 Changes in nuclear bond energy data during the decay o f $^{12}C^*$.

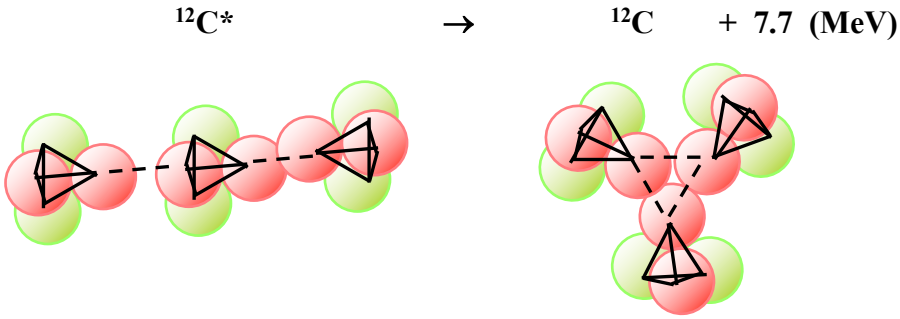

Figure 4.2. Changes in nuclear bond model of the ground state of ^{12}C.

4.2 Bethe's C-N-O Cycle

Bethe [1938] used known Eb and Ex data for the following nuclei to account for the spectra of pulsating giant stars often observed in old globular clusters.

He showed that these nuclei react cyclically to produce helium, energy and some oxygen.

^{12}C, $^{12}C^*$, ^{13}C, ^{13}N, $^{13}N^*$, ^{14}N, $^{14}N^*$, ^{15}N, ^{15}O , ^{15}O *, ^{16}O and $^{16}O^*$.

Many of the fusions involve resonan reactions resulting in excited nuclei which quickly lose their excitation energy as gamma rays. Essentially Bethe's theory involves the fusion of four protons into a helium nucleus with carbon acting as a catalyst. For this reason the reaction is often known as the nuclear 'carbon cycle' and may be written as follows:

$$^{12}C + {}^{1}H \rightarrow {}^{13}N + \gamma$$
$$^{13}N \rightarrow {}^{13}C + \beta^+ + \nu_e$$
$$^{13}C + {}^{1}H \rightarrow {}^{14}N + \gamma$$
$$^{14}N + {}^{1}H \rightarrow {}^{15}O + \gamma$$
$$^{15}O \rightarrow \beta^+ + {}^{15}N + \nu_e$$
$$^{15}N + {}^{1}H \rightarrow {}^{12}C + {}^{4}He$$

In effect this cycle consists of four proton captures, three gamma emissions, two β^+ decays and an alpha decay. The following Figure has been made in terms of the nuclear bond structures of all nuclei involved in the cycle.

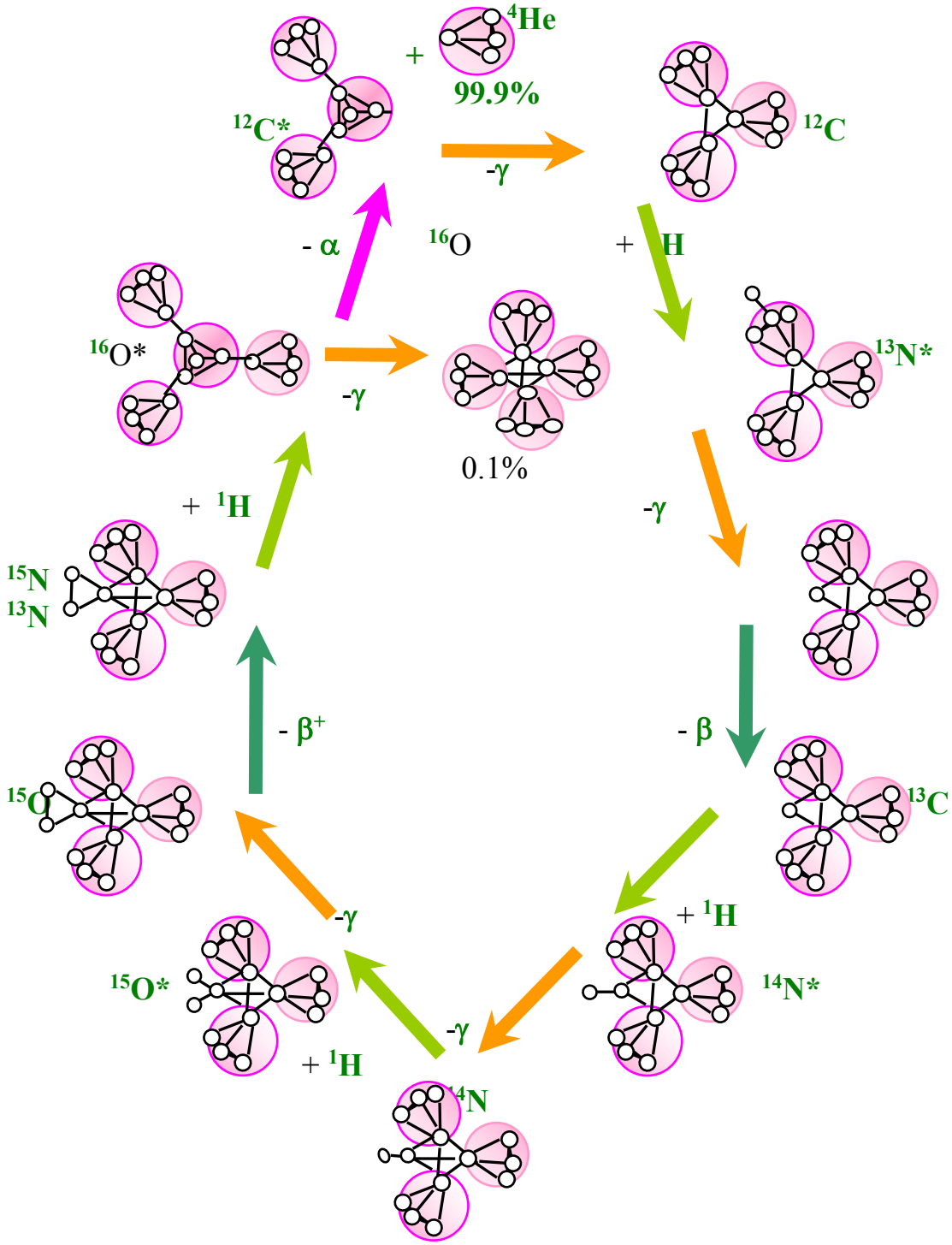

Figure 4.3 A nuclear bond model of Bethe's C-N-O cycle.

	Nucleus	Origin	E_x (MeV)	E_b (MeV)	E_c (MeV)	E_n (MeV)	(NB) Total	(NB)in alphas	(NB)ex alphas
1	^{12}C **98.89%**	$^{8}Be+^{4}He\rightarrow$ $^{12}C^{*}\rightarrow$ ^{12}C		92.2	8.1	100.3	20.7	3 x 6	3x0.9
	$^{13}N^{*}\rightarrow$ $^{13}N + E_x$	$^{12}C+^{1}H\rightarrow$ $^{13}N^{*}$	2.4	91.7	10.3	102.0	21.1	3 x 6	3x0.9 +1x0.4
2	$^{13}N\rightarrow$ $\beta^{+} + {}^{13}C$	$^{13}N^{*}\rightarrow$ $^{13}N + E_x$	-	94.1	11.1	105.2	21.8	3 x 6 x 1	3 x 0.9 +2x 0.5
	^{13}C **1.11%**	$^{13}N\rightarrow$ $\beta^{+} + {}^{13}C$	-	97.1	8.1	105.2	21.7	3 x 6	3 x 0.9 +2x 0.5
3	$^{14}N^{*}\rightarrow$ $^{14}N + E_x$	$^{13}C+^{1}H\rightarrow$ $^{14}N^{*}$	8.0	96.7	11.1	107.8	22.3	3 x 6	3x0.9+ 3x0.5
	^{14}N 99.63%	$^{14}N^{*}\rightarrow$ $^{14}N + E_x$	-	104.7	11.4	116.1	24.0	3 x 6	6x0.9+ 1x0.5
4	$^{15}O^{*}\rightarrow$ $^{15}O + E_x$	$^{14}N+^{1}H\rightarrow$ $^{15}O^{*}$		104.4	14.4	118.8	24.7	3 x 6	6x0.9+ 2x0.6
	$^{15}O\rightarrow$ $\beta^{+} + {}^{15}N$	$^{15}O^{*}\rightarrow {}^{15}O +$ E_x	-	112.0	14.9	126.9	26.3	3 x 6	9x0.9
5	^{15}N 0.37%	$^{15}O\rightarrow$ $\beta^{+} + {}^{15}N$	-	115.5	11.4	126.9	26.2	3 x 6	9x0.9
	$^{16}O^{*}\rightarrow$ $^{12}C^{*}+^{4}He$	$^{15}N+^{1}H\rightarrow$ $^{16}O^{*}$	12.4	115.2	14.0	129.2	26.7	4 x 6	3x0.9
6	$^{16}O^{*}\rightarrow$ $^{16}O+E_x$	$^{15}N+^{1}H\rightarrow$ $^{16}O^{*}$	12.4	115.2	14.0	129.2	26.7	4 x 6	3x0.8
	^{16}O 99.76%	$^{16}O^{*}\rightarrow$ $^{16}O+ E_x$	-	127.6	14.9	142.5	29.5	4 x 6	6 x 0.9
7	^{4}He 99.99%	$^{16}O^{*}\rightarrow$ $^{12}C^{*}+^{4}He$	-	28.3	0.8	29.1	6.0	6	-
	$^{12}C^{*}\rightarrow$ $^{12}C+ E_x$	$^{16}O^{*}\rightarrow$ $^{12}C^{*}+^{4}He$	4.4	87.8	7.4	95.2	19.7	3 x 6	2x0.9

Table 4.3 Changes in nuclear bond energy data during the C-N-O cycle.

The data in the far right column indicates the probable bond structure of the nuclei as depicted in Fig. 4.3.

It is important to note that the nuclear bond model of ^{16}O in its ground state is a tetrahedral cluster of 4 alphas tightly bound by 6 (NB). Furthermore, it will soon become apparent that this structure forms the core of all heavier nuclei! As such, these 4 alphas form the first of a total of 6 such layers to model ^{238}U.

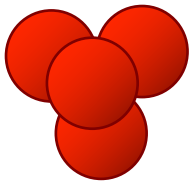

Figure 4.4 A simple model of ^{16}O.

It will also become apparent that the stability of each of the 6 nuclei with a closed outer layer is usually one of the more abundant nuclei in the chart of solar system abundances in Fig.4.5.

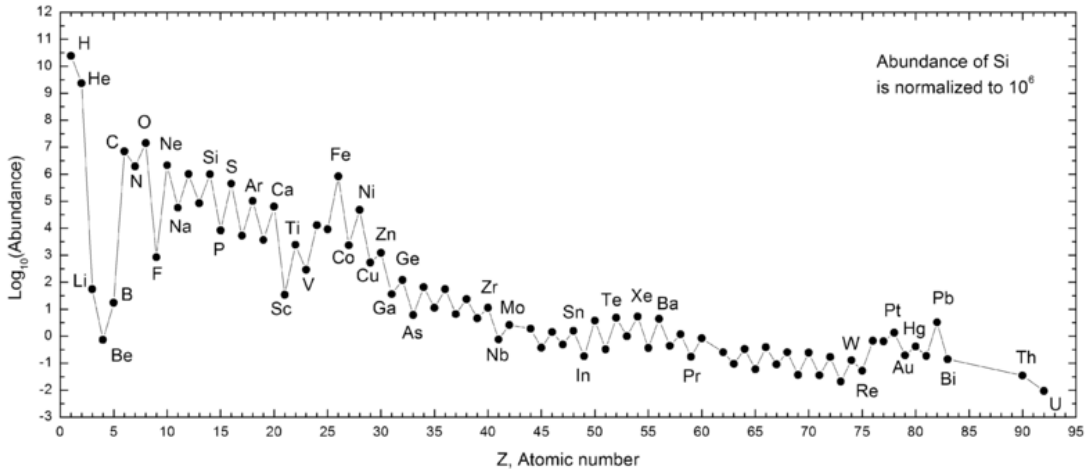

Figure 4.5 Relative abundance of elements in the solar system.

Chapter 5. Synthesis of nuclei up to nickel in heavy stars

5.1 Synthesis of nuclei up to sulphur

When the core temperature reaches $1x10^9$ K following further core collapse photodisintegration of ^{20}Ne produces ^4He and ^{16}O nuclei because of the relatively weak bonding between them: $^{20}Ne \rightarrow {}^4He + {}^{16}O - 4.8$ (MeV)

Some of these alphas then fuse with undissociated ^{20}Ne nuclei to form ^{24}Mg nuclei:

$$^4He + {}^{20}Ne \rightarrow {}^{24}Mg + 8.2 \text{ (MeV)}$$

At the conclusion of neon burning the core collapses thereby raising the temperature to $2x10^9$ K when oxygen burning produces mostly silicon and sulphur.

Nucleus	Eb (MeV)	Ec (MeV)	En (MeV)	Bond Total (NB)	Bonds in alphas (NB)	Bonds ex alphas (NB)
^{20}Ne	160.7	22.2	182.9	37.8	30 = 5x6	7.8= 6+ 3x0.6
^{24}Mg,	197.2	30.7	227.9	47.1	36 = 6x6	11.1= 6+2 x3x 0.9
^{28}Si	236.5	40.2	276.7	57.2	42 = 7x6	15.2= 6+3x3x1 .
^{32}S	271.8	50.7	322.5	66.6	48 = 8x6	18.6=6+4 x3x 1

Table 5.1 Energy data for ^{20}Ne, ^{24}Mg, ^{28}Si and ^{32}S nuclei.

It is evident from Table 5.1 that each of these nuclei may be considered as the result of binding an extra alpha to the central oxygen nucleus by 3 (NB). In order to bind each extra alpha closely to the oxygen core they bind to each of the 4 faces of the tetrahedron thereby forming an almost spherical second layer as ^{32}S. Each of the 3 (NB) binds with a different alpha of the face.

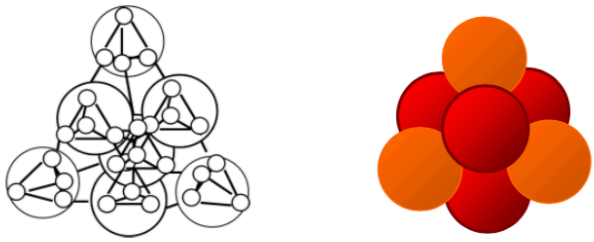

Figure 5.1 Nuclear bond models of the ^{32}S nucleus.

5.2 Synthesis of nuclei up to nickel

Smaller amounts of argon and calcium as well as chlorine, potassium and nuclei up to the neighborhood of scandium are produced in a complicated network of reactions produced by oxygen burning according to Woosley et al [1972, 1978]

Collapse of the core crushes some silicon nuclei releasing alphas which react with silicon, sulphur, argon and calcium to eventually form nickel and iron as outlined by Rolfs and Rodney [1988]. It has been estimated that oxygen burning lasts only several months before silicon burning begins. This lasts for only a few days before the core collapses producing a shock wave resulting in a brief burst of X rays. Such a burst was recently observed by Sodenberg [2008] as a Wolf-Rayet star became a type Ib supernova known as SN2008D.

Nucleus	E_b (MeV)	E_c (MeV)	E_n (MeV)	Bond total (NB)	Bonds in alphas (NB)	Bonds ex alphas (NB)
^{40}Ca 97.0%	342.1	74.4	416.5	86.1	60 = 10 x 6	26 =6 + 12 +2x4
^{52}Cr 83.8%	456.3	99.1	555.4	114.2	72 = 12 x 6	42 =6 +12 +4x4+4x 2
^{56}Ni → ^{56}Co + β^+	483.7	132.4	616.1	127.3	84 = 14 x 6	43 =6 + 12 +6x4

Table 5.2 Energy data for ^{40}Ca, ^{52}Cr and ^{56}Ni nuclei.

The synthesis of a ^{35}Cl nucleus effectively involves the addition of a triton to a ^{32}S nucleus. These two nuclei are firmly bound by 4 (NB). It is noteworthy that most nuclei heavier than ^{32}S have a third layer of alphas each attached to the first layer of ^{16}O by 4 (NB). Each of these bonds is bound to an outer nucleon of an alpha in the first layer as illustrated in Fig.5.2 . Each additional alpha in the third layer is close-packed to one of the 6 edges of the tetrahedron.

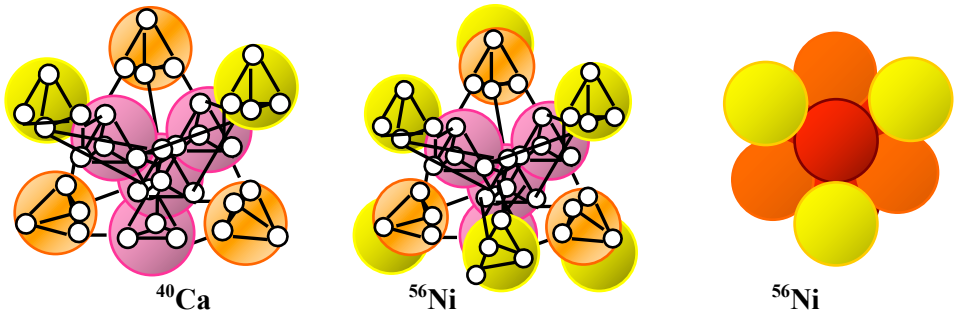

Figure 5.2 Nuclear bond models of the calcium 40 and nickel 56 nuclei.
The first layer of alphas is coloured red, the second is orange and the third layer is yellow.

Layer in Nucleus	Alphas in Layer	Bonds in Layer (NB)	Bonds ex Layer (NB)	Bonds in+ex Layer (NB)	Nucleus
1	4	4 x 6 = 24	4 x 3/2 x 0.9 = 5.4	29.4	^{16}O
2	4	4 x 6 = 24	4 x 3 x 1 = 12	36	^{32}S
3	6	6 x 6 = 36	6 x 4 x 1 = 24	60	^{56}Ni

Table 5.3 The first 3 alpha layers of nuclei synthesized in supergiant stars.

Each of the burnings (fusions) outlined above produces denser nuclei as the core shrinks and gets hotter so that a series of concentric shells of reactions proceed as shown in Fig. 5.3

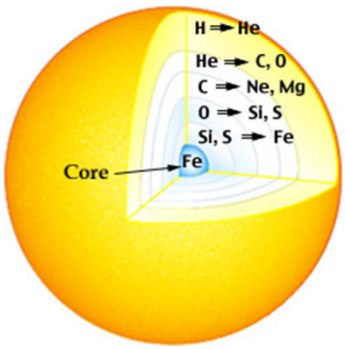

Figure 5.3 The internal shell structure of a heavy star

Chapter 6. Synthesis of all nuclei in a supernova.

6.1 A Supernova

It transpires that ^{56}Ni is unstable as it begins to radiate positrons as it decays into unstable ^{56}Co which further decays into ^{56}Fe. Their respective half-lives are 6 and 77 days because of the dominance of ΔEc over ΔEn as shown in Table 6.1.

Nucleus	**^{56}Ni →**	**e^+ +**	**^{56}Co**	**Energy change**
Energy	**A**	**B**	**C**	**ΔE = B + C - A**
Eb (MeV)	483.7	-	486.9	**ΔEb = 3.2 (MeV)**
+ Ec (MeV)	132.4	-	122.9	**+ ΔEc = - 9.5 (MeV)**
= En (MeV)	616.1	-	609.8	**= ΔEn = - 6.3 (MeV)**
= En (NB)	127.1=30+ 36+60	- -	126.0=30+36+59	**= ΔEn = -1.1 (NB)**

Nucleus	**^{56}Co →**	**e^+ +**	**^{56}Fe**	**Energy change**
Energy	**C**	**B**	**C**	**ΔE = B + C - A**
Eb (MeV)	486.9	-	492.3	**ΔEb = 5.4 (MeV)**
+ Ec (MeV)	122.9	-	113.8	**+ ΔEc = - 9.1 (MeV)**
= En (MeV)	609,8	-	606.1	**= ΔEn = - 3.7 (MeV)**
= En (NB)	126.0=30+36+59	-	125.2=30+36+58	**= ΔEn = - 0.8 (NB)**

Table 6.1 Energy data of the beta decays of ^{56}Ni and ^{56}Co

Both of these positron decays occur because Coulomb repulsion breaks a nuclear bond. That is, ΔEb = - ΔEc + ΔEn. Because of the increasing dominance of Ec in heavy nuclear structures it is found that iron is the most stable nucleus with the largest binding energy per nucleon. For this reason the core of the super-giant star is unable to support the weight of the outer shells of fusing elements so there is a violent implosion, seen as a supernova.

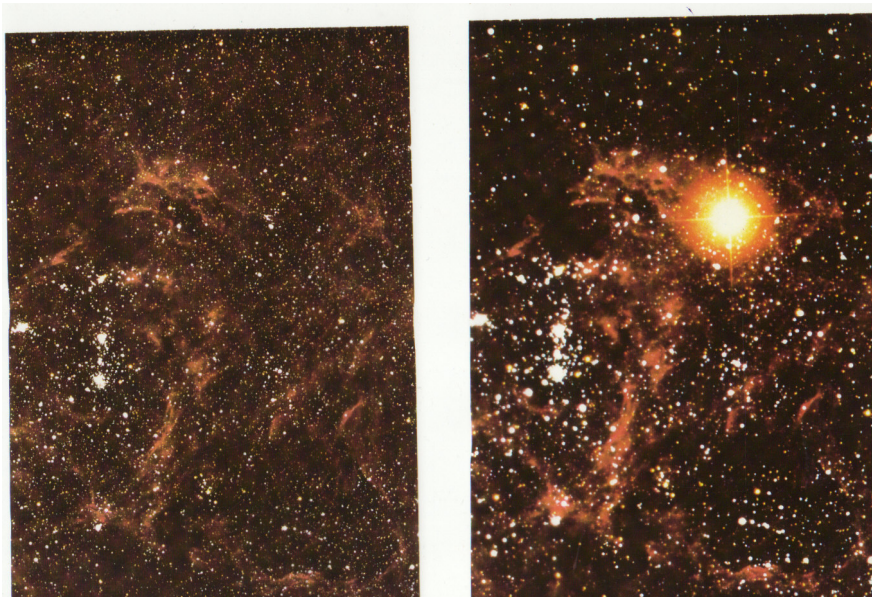

Figure 6.1 Large Magellan Cloud before and after explosion

In 1987 the blue supergiant Sanduleak in the Large Magellan Cloud suddenly exploded in this way as the core was crushed to a dense sphere of neutrons only 10 km in diameter..This core spins incredibly quickly despite having a mass of 1.4 suns. As it collapsed it radiated much energy as neutrinos and ever since as synchrotron radiation so that it is detected as a pulsar.

The implosion of the core created a shock wave that ejected a large spherical layer of ight nuclei that were rapidly fused into ^{56}Ni by the heat of the shock wave. At the same time a very dense flux of neutrons resulted in the synthesis of all heavier nuclei up to uranium and beyond. The details of these fusions are outlined in the rest of this chapter.

It was the simultaneous release of all this energy that alerted astronomers to the event. One of them, Bruce Tregaskis, a senior electrical engineer and amateur variable star observer regularly recorded the apparent brightness of SN 1987A for many months. His data was then plotted by senior chemist, Dr.Peter Skilton as in Fig. 6.2.:

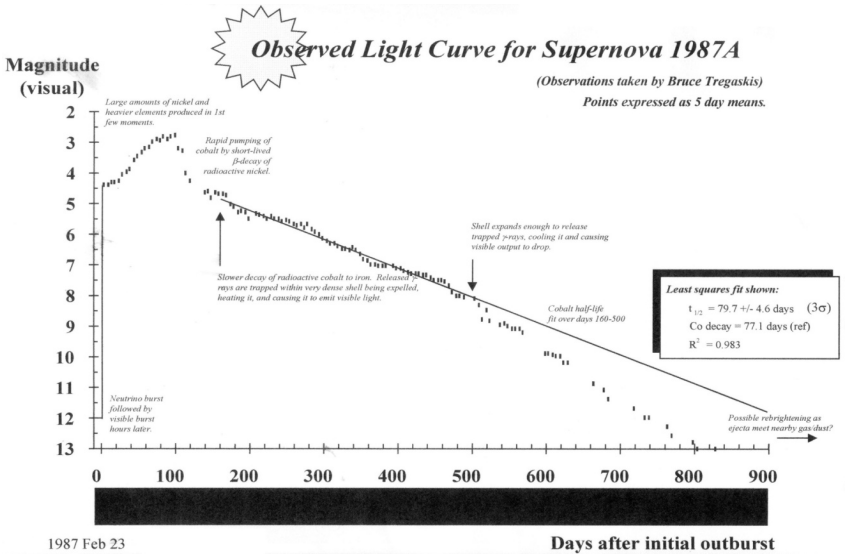

Figure 6.2 Light curve of Supernova 1987 A

It is noteworthy that this accurate light curve demonstrates the beta decays of both ^{56}Ni and ^{56}Co with half-lives of 6 and 77 days respectively .

6.2 Synthesis of nuclei up to tellurium

Because of the increasing dominance of the Coulomb repulsion with increasing proton numbers it has been shown that heavy nuclei are synthesised by the fusion of 4 or more neutrons followed by the radiation of an electron so that the next stable heavy nucleus is formed as shown im Fig. 6.3, from Thielemann, [1983]

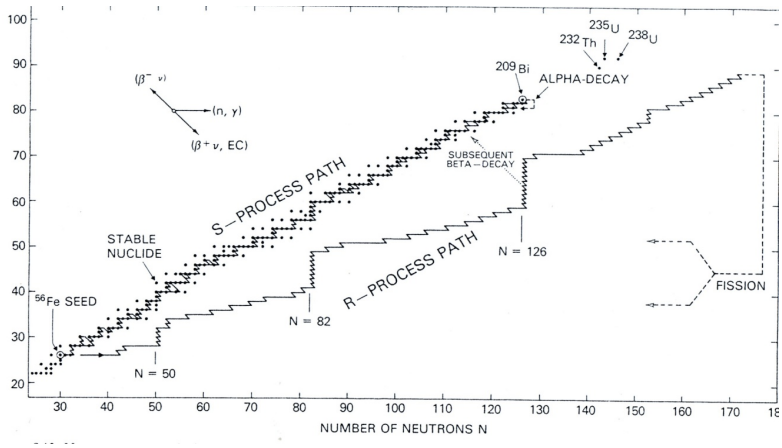

Figure 6.3 Chart of nucleosynthesis of heavy nuclei

It is significant that all stable nuclei heavier than calcium have a thin skin of non-repulsive neutrons to provide more stabilising nuclear bond energy. Several examples listed above are stable ^{52}Cr and ^{56}Fe each with a skin of 4 neutrons . By contrast, both ^{56}Ni and ^{56}Co are unstable. However, ^{60}Ni is stable with a skin of 4 neutrons.

Nucleus [skin]	Eb (MeV)	Ec (MeV)	En (MeV)	Bond total (NB)
$^{60}Ni_{28}$ [4]	526.8	129.4	656.2	135.6
$^{74}Ge_{32}$ [10]	645.6	158.3	803.9	166.1
$^{84}Kr_{36}$ [12]	732.2	192.8	925.0	191.1
$^{90}Zr_{40}$ [10]	783.	233.2	1017.1	210.2
$^{102}Ru_{44}$ [14]	877.9	271.3	1149.2	237.4
$^{114}Cd_{48}$ [18]	972.5	311.7	1284.2	265.32
$^{130}Te_{52}$ [26]	1095.9	352.7	1448.6	299.3

Table 6.2a Energy data of ^{60}Ni and some of the stable nuclei in layer 4

Layers	3	4	4	4	4	4	4
Element	$^{60}Ni_{28}$	$^{74}Ge_{32}$	$^{84}Kr_{36}$	$^{90}Zr_{40}$	$^{102}Ru_{44}$	$^{114}Cd_{48}$	$^{130}Te_{52}$
Alphas in layer	6	2	4	6	8	10	12
(NB) in layer	6x6=36	2x6=12	4x6=24	6x6=36	8x6=48	10x6=60	12x6=72
(NB) ex layer	6x4=24	2x4=8	4x4=16	6x4=24	8x4=32	10x4=40	12x4=48
(NB) in+ex layer	60	20	40	60	80	100	120
(NB) in core + layer	66+60 = 126	126+20= 146	126+40 =16 6	126+60 = 186	126+80 = 206	126+100 = 226	126+120 = 246
Neutrons in skin	4	10	12	10	14	18	26
(NB) ex skin	4x2 = 8	10x2=20	12x2=24	10x2 = 20	14x2 = 28	18x2 = 36	26x2=52
Total (NB) in Model	134	146+20 = 166	166+24 = 190	186 + 20 =206	206 + 28 = 234	226 + 36 = 262	246+52 = 298
Total (NB) from Data	136	166	191	210	237	265	299

Table 6.2b Nuclear Bond Models of closed layer Nuclei $^{60}Ni_{28}$ and $^{130}Te_{52}$

Note that the core of ^{60}Ni is ^{32}S. Tables 6.2 a&b show that in the fourth layer of 12 alphas each alpha is bound to the inner layers by 4 (NB). Furthermore, the neutron skin gradually grows to balance the increasing Coulomb repulsion until ^{130}Te with an extra neutron bound to each of the 26 --alphas. Each skin neutron is bound by 2 (NB). It is interesting tonote that each of these simple bond models agrees with the energy data to within 2%.

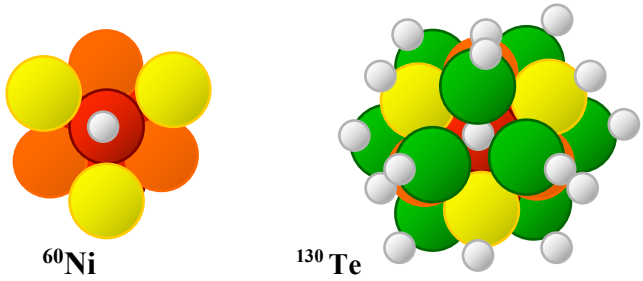

Figure 6.4 Nuclear bond models of ^{60}Ni and ^{130} Te

6.3 Synthesis of nuclei up to osmium

As the atomic number of nuclei increases there is an approximately proportional increase in the number of neutrons in the skin as shwn in Fig.6.5.

54																			U
52													8	α	of			Th	
50													Lay	er	6		Rn	Ra	
48																			
46																			
44															Pb	Po			
42														Hg					
40													Pt						
38												Os							
36			12	α	of						W								
34			Lay	er	5					Hf									
32						Gd	Dy	Er	Yb										
30																			
28					Sm														
26		Ba																	
24	Xe		Ce																
22				Nd															
20																			
18																			
16																			
14																			
12																			
10																			
8																			
6																			
4																			
2																			
0																			
α	27	28	29	30	31	32	33	34	35	36	37	38	39	40	41	42	43	44	45	46

Figure 6.5 Chart of skin neutron numbers relative to alpha numbers

Nucleus (skin)	Eb (MeV)	Ec (MeV)	En (MeV)	Bond Total (NB)
$^{138}Ba_{56}$ (26)	1158.3	399.7	15576	321.8
$^{142}Nd_{60}$ (22)	1185.1	454.6	1639.7	338.8
$^{158}Gd_{64}$ (30)	1295.9	499.7	1795.5	371.0
$^{166}Er_{68}$ (30)	1351.6	555.0	1906.6	393.9
$^{180}Hf_{72}$ (36)	1446.3	606.2	2052.5	424.1
$^{190}Os_{76}$ (38)	1512.7	660.9	21736	449.1

Table 6.3 Energy data of some of the stable nuclei in layer 5

Layers	4	5	5	5	5	5	5
Element	$^{130}Te_{52}$	$^{138}Ba_{56}$	$^{142}Nd_{60}$	$^{158}Gd_{64}$	$^{166}Er_{68}$	^{76} $^{180}Hf_{72}$	$^{190}Os_{76}$
Alphas in layer	12	2	4	6	8	10	12
(NB) in layer	12x6=72	2x6=12	4x6=24	6x6=36	8x6=48	10x6=60	12x6=72
(NB) ex layer	12x4=48	2x5=10	4x5=20	6x5=30	8x5=40	10x5=50	12x5=60
(NB) in+ex layer	120	22	44	66	88	110	132
(NB) in core + layer	126+120 = 246	246+22= 268	246+44 =290	246+66 = 312	246+80 = 334	246+110 = 356	246+13 2 = 378
Neutrons in skin	26	26	22	30	30	36	38
(NB) ex skin	26x2=52	26x2=52	22x2=44	30x2 = 60	30x2 = 60	36x2 = 72	38x2=76
Total (NB) in Model	246+52 = 298	268+52 = 320	290+44 = 334	312 + 60 =372	334+ 60 = 394	356+ 72 = 428	378+576= 454
Total (NB) from Data	299	321	339	371	3943	424	449

Table 6.3. Nuclear Bond Models of closed layer Nuclei $^{130}Te_{52}$ to $^{190}Os_{76}$

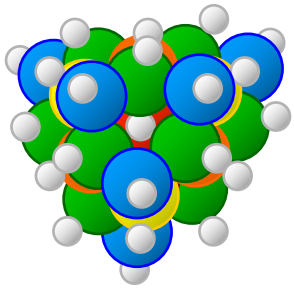

Figure 6.6 Nuclear bond model of ^{190}Os

As indicated in Table 6.3, each of the 12 alphas of layer 5 is bound to the inner layers by 5 (NB). Each extra **skin** neutron stabilises the nucleus by the provision of approximately 2 (NB). This layer is complete in ^{190}**Os** which is unique in having a skin- neutron for each of the 38 alphas as shown in Fig.6.6.

6.4 Synthesis of nuclei up to uranium

Many isotopes of elements in layer 5 are unstable because of the increasing of the long-range Coulomb repulsion over the short-range nuclear attraction so it is no surprise that only 8 elements form layer 6. Energy data for several nearly stable elements of this layer are in Table 6.4.

Nucleus (skin)	**Eb (MeV)**	**Ec (MeV)**	**En (MeV)**	**Bond Total (NB)**
$^{200}Hg_{80}$ **(40)**	1581.2	723.820	23050	476.2
$^{210}Po_{84}$ **(42)**	1645.3	786.0	2431.3	502.3
$^{226}Ra_{88}$ **(50)**	1731.6	847.0	2578.6	532.65
$^{238}U_{92}$ **(54)**	1801.7	905.1	2706.7	559.2

Table 6.4 Energy data of some of the "stable" nuclei in layer 6

Layers	5	6	6	6	6
Element	$^{190}Os_{76}$	$^{200}Hg_{80}$	$^{210}Po_{84}$	$^{226}Ra_{88}$	$^{238}U_{92}$
Alphas in layer	12	2	4	6	8
(NB) in layer	12x6=72	2x6=12	4x6=24	6x6=36	8x6=48
(NB) ex layer	12x5=60	2x5=10	4x5=20	6x5=30	8x5=40
(NB) in+ex layer	132	22	44	66	88
(NB) in core + layer	246+132 = 378	378+22 =4 v00	378+44 =422	378+66 = 444	378+80 = 466
Neutrons in skin	38	40	42	50	54
(NB) ex skin	38x2=76	40x2 =80	42x2=84	44x2 +6x1= 94	46 x 2 +8x1= 1000
Total (NB) in Model	378+576= 454	400+80 = 480	422+84 = 506	444 + 94 =538	466+ 100 = 566
Total (NB) from Data	449	476 ??	**502**	**532.**	**559**

Table 6.4. Nuclear Bond Models of some closed layer Nuclei from $^{190}Os_{76}$ to $^{238}U_{92}$

The data shows that the inner layers remain unchanged and each new alpha is bound by 5 (NB).
The nuclei of layer 6 are so unstable that they are among the least abundant in the universe. Quite a few heavier nuclei have been formed but their decay times are very short.

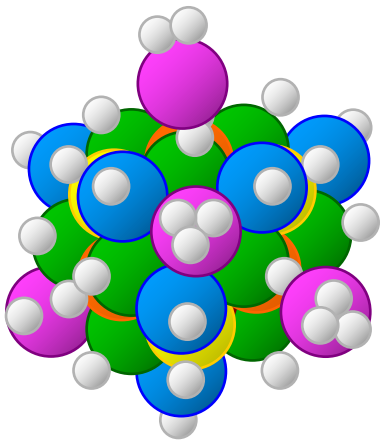

Figure 6.7 Nuclear bond model of ^{238}U

Table 6.5 combines the 6 nuclear bond models of closed layer nuclei and demonstrates not only the regularity of the alpha array but also that of the nuclear bonds. It seems in Table 6.5 that each extra alpha of ^{238}U is only stabilised by the addition of two neutrons each held by only 1(NB) as indicated by the model of ^{238}U in Fig.6.7. Incidentally, the last two rows of the Table show how little variation there is between the number of nuclear bonds in each model and those from the data.

It should be noted that each of the 6 nuclei involved is not only the most stable and abundant isotope of its element but also more abundant than its neighbouring elements.
Models of nuclei with an odd number of protons have rarely been discussed but they have a regular underlying alpha structure.

Layers	1	2	3	4	5	6
Alphas in layer	4	4	6	12	12	8
(NB) in layer	4x6=24	4x6=24	6x6=36	12x6=72	12x6=72	8x6=48
(NB) ex layer	4x3/2=6	4x3=12	6x4=24	12x4=48	12x5=60	8x5=40
(NB) in+ex layer	30	36	60	120	132	88
Closed layer Nuclei	^{16}O	^{32}S	^{60}Ni	^{130}Te	^{190}Os	^{238}U
(NB) in core	30	30+36 =66	66+60 = 126	126+120 = 246	246+132 = 378	378+88 = 466
Neutrons in skin	-	-	4	26	38	54
(NB) ex skin	-	-	4x2 = 8	26x2 = 52	38x2 = 76	76+16x1 =92
Total (NB) in Model	30	66	134	298	454	558
Total (NB) from Data	29	67	136	299	450	559

Table 6.5. Nuclear Bond Models of closed layer Nuclei

Chapter 7. Dying Stars

7.1 White Dwarfs

Solar Death as a White Dwarf

The sun is now a typical middle weight and middle aged stable star about 5 Gy old. After another 5 Gy it will have fused most of its hydrogen into helium. With insufficient weight to form heavier nuclei, the sun will become an unstable red giant as it expands. After reaching Mars it will shrink and become a white dwarf star with a radius only 1% of its present value - that is, the Sun will shrink to the size of the Earth! The dense core will consist of compressed degenerate electrons. The surface will then appear a dim white. Eventually, as the residual energy escapes, the dwarf will turn yellow then red until it ends as a cold black dwarf.

Red Giant to White Dwarf or Supernova?

Low-mass red giants end up as pulsating nebulae, gently puffing off their distended atmospheres of hydrogen at low velocities and leaving their dense cores of carbon as white dwarfs to cool and shrink forever.
By contrast, more massive red giants have sufficient gravitational energy to convert some of the carbon into the heavier nuclei ^{16}O, ^{20}Ne, ^{24}Mg, ^{28}Si, ^{32}S, ^{40}C and ^{56}Fe at which stage they become unstable and explode violently as super-novae as explained earlier.

Diamond Star Lucy and Sirius B.

On Valentine's Day in 2004 Dr. Metcalfe at the Harvard-Smithsonian Centre for Astrophysics announced the discovery of an old, cold white dwarf star with a highly compressed core of diamond. This star, known as BPM 37093, is 50 light years distant in the constellation of Centaurus. It began life as a middle-weight star about 12 billion years ago and 2 billion years ago it became a red giant as it synthesized carbon in its core. As it cooled it gradually compressed the carbon into diamond so that it now has the properties outlined in Table 7. 1 where it is compared with the nearer and younger white dwarf, Sirius B.

	Dia**mond Star Lucy**	**Sirius B**
Diameter	4,000 km = 0.001 sun	56,000 km = 0.02 sun
Mass	10^{34} carats = 1 sun	1 sun
Distance	50 light years	8.7 light years
Composition	90% diamond	90% carbon
Constellation	Centaurus	Canis Major
Name	BPM 37093	α CMa B
Age	12 G years	10 G years

Table 7.1. Properties of Diamond Star Lucy and Sirius B

7.2 Neutron stars and Pulsars

If the core of a supernova is more massive than 1.4 suns it compresses protons and degenerate electrons into neutrons so that the density is about 10^{14} tonne per cubic metre. The conserved angular momentum causes the neutron star to rotate very rapidly. Pulsars are those neutron stars that radiate radio waves and/or light or X and gamma rays that are detected at rates ranging from 0.3 to 5,000 pulses per second as determined by the spin rate of the neutron star. The Crab nebula appeared in 1054 when a super-giant star exploded as a supernova. At its centre is an optical pulsar.

7.3 Black Holes

If the mass of the core of a super-giant supernova is more massive than 4 suns it collapses until so dense that even light is unable to escape the incredibly powerful gravity. Furthermore, such black holes can acquire more mass by capturing nearby objects. In this way some have grown to be millions of times more massive than the sun. Such black holes are the cores of huge galaxies. One such giant is Sagitarius A* at the centre of the Milky Way. Despite being invisible it was deduced from the rapid orbital movements of neighbouring stars.

Chapter 8. Nuclear Bond Energetics

8.1 Nuclear Fusion

Fusion occurs when 2 or more reactants fuse to form a single product. The reactants are nucleons and/or nuclei when nuclear fusion occurs.

As each fusion occurs free energy is released as mass decreased as ΔEn is larger than ΔEc.

8.2 Excited light nuclei

Ikeda [1967] showed that as even-even light nuclei were excited, their tight nuclear structures seemed to gradually unravel into less strongly bound chains of alphas in the manner of a drop of viscous liquid stretching under the influence of gravity.

As these excited nuclei relax by radiating gamma rays they eventually each resume the tightly bound ground state. The simplest excited nucleus to display this behaviour is $^{12}C^*$, first predicted to exist by Hoyle [1953], the cosmologist.
The nuclear bond data and related diagrams of excited states of ^{12}C, ^{16}O, ^{328}Si and ^{32}S are shown in Table 8.1 and Fig. 8.1. Norman [2003] has previously published similar information for ^{20}Ne and ^{24}Mg based on Ikeda's work.

Energy Nucleus	Ex (MeV)	Eb (MeV)	+ Ec (MeV)	= En (MeV)	= En (NB)	= (NB) In alphas	+ (NB) Between alphas
^{12}C	-	92.1	8.8	100.9	20.8	18.0	3 x 0.9
$^{12}C^*$	7.3	84.8	7.2	92.0	19.0	18.02	2 x 0.5
^{16}O	-	127.6	14.9	142.5	29.4	24	6 x 0.9
$^{16}O^*$	7.2	120.4	12.7	133.1	27.5	24.0	4 x 0.9
$^{16}O^{**}$	14.4	113.2	11.4	124.6	25.7	24.0	3 x 0.6
$^{28}Si^{***}$	24.0	212.5	31.6	244.1	50.4	42.0	9 x 0.9
$^{32}S^{****}$	31.0	240.8	37.7	278.5	57.5	48	10 x 1.0

Table 8.1. Energy and Nuclear Bond data for some light stable and excited nuclei.

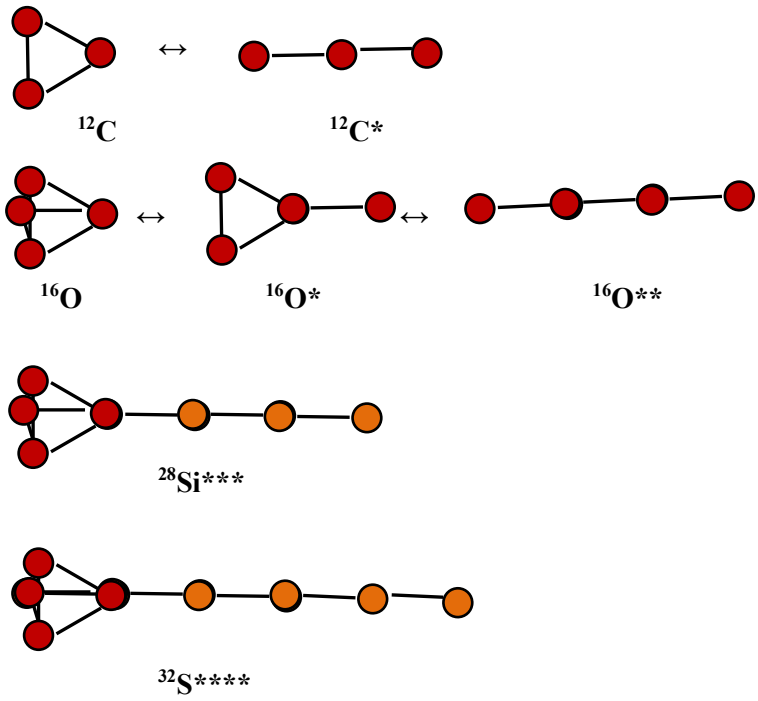

Figure 8.1. Nuclear bond models of ^{12}C, $^{12}C^*$,^{16}O, $^{16}O^*$ $^{16}O^{**}$,$^{28}Si^{***}$ and $^{32}S^{****}$

Nucleus	$^{16}O + \Delta Ex \rightarrow$	$^{16}O^*$	Energy change
Energy	A	B	ΔE = B - A
Eb (MeV)	127.6	120.4	ΔEb = - 7.2 (MeV) = ΔEx
+ Ec (MeV)	14.9	12.7	$+\Delta Ec$ = - 2.2 (MeV)
= En (MeV)	142.6	133.1	= ΔEn = - 9.4 (MeV)
= En (NB)	29.42	27.5	= ΔEn = - 1.9 0 (NB)

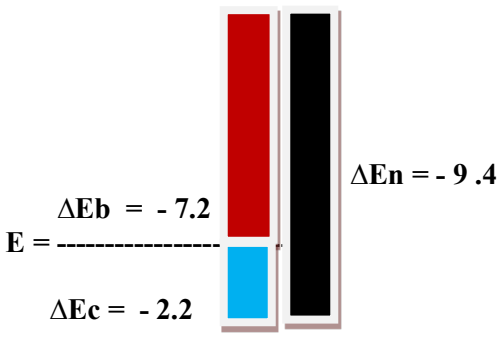

Table 8.2. Nuclear energy changes when ^{16}O is excited to $^{16}O^*$.

8.3 Radioactive decay.

Alpha decay

Nuclear decay is a form of nuclear fission which is the reverse of fusion. One reactant decays to two or more products as ΔEc decreases more than Δ En.

Alpha decay occurs in some unstable isotopes of some layer 5 elements and in even less stable isotopes of most layer 6 elements. Relevant data and models are in Table 8.2 and Fig.8.2. More data shows that usually 6 or 5 (NB) are broken per decay.

Nucleus	**^{238}U →**	**^{4}He +**	**^{234}Th**	**Energy change**
Energy	**A**	**B**	**C**	**ΔE = B + C - A**
Eb (MeV)	1801.6	28.3	1777. 6	**ΔEb = 4.3 (MeV)**
+ Ec (MeV)	905.1	0.8	870.9	**+ΔEc = - 33.4 (MeV)**
= En (MeV)	2706.7	29.1	2648.5	**= ΔEn = - 29.1 (MeV)**
= En (NB)	559	6	547	**= ΔEn = - 6 (NB)**

Table 8.3. Energy data for alpha decay from layers 6.

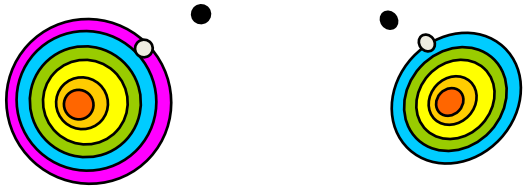

Figure 8.2 . Cross sections of alpha decay from layers 6 and 5.

Beta decay

Beta decay occurs when an unstable nucleus changes into a more stable nucleus of a neighbour element with the same number of nucleons. The two types of beta decay are beta $^{+}$ and beta^{-}

Beta $^{+}$ decay

If an isotope of an element is unstable because it has less neutrons than the stable isotope, it will radiate a positron (positive electron) and an electron anti-neutrino. This decay effectively changes a proton into a neutron thereby reducing the repulsive Coulomb energy to a more tolerable level.

The example shown in Table 8.3 is of the positron decay of ^{11}C which is used in positron emission tomography (PET scanning).

Significantly the role of Coulomb repulsion in this decay is demonstrated by the large decrease in Ec.

Nucleus	**^{11}C →**	**e + +**	**^{11}B**	**Energy change**
Energy	**A**	**B**	**C**	**ΔE = B + C - A**
Eb (MeV)	73.4	-	76.2	**ΔEb =** 2.8 (MeV)
+ Ec (MeV)	9.0	-	6.0	**+ΔEc** = - 3.0 (MeV)
= En (MeV)	82.4	-	82.2	**= ΔEn** = - 0.2 (MeV)
= En (NB)	17.02	-	16.98	**= ΔEn = - 0.04** 0 (NB)

Table 8.3. Energy data for beta^{+} decay of ^{11}C

Beta $^{-}$ decay

This type of decay occurs in isotopes with more neutrons than required for stability. They therefore emit a negative electron and an electron neutrino. In this case the small increase of mass and nuclear bond energy is supplied by the increased Coulomb energy.

The decay shown in Table 8.4 is used in carbon dating plant and animal fossils.

Nucleus	**^{14}C →**	**e^{-} +**	**^{14}N**	**Energy change**
Energy	**A**	**B**	**C**	**ΔE = B + C - A**
Eb (MeV)	105.2	-	104.7	**ΔEb = - 0.5 (MeV)**
+ Ec (MeV)	8.3	-	11.7	**+ΔEc = 3.4 (MeV)**
= En (MeV)	113.5	-	116.4	**=ΔEn = 2.9 (MeV)**
= En (NB)	23. 5	-	24.0	**=ΔE n = 0.5 (NB)**

Table 8.4. Energy data for beta^{-} decay of ^{14}C

8.4 Nuclear Fission

The combined product yields by mass for thermal neutron fission of ^{235}U and ^{239}Pu is given in Fig.8.3. The light daughter never has less than three alpha layers and the heavy daughter never has less than 4 alpha layers. The outer layer(s) are separated (like egg white) from the stronger core (egg yolk).

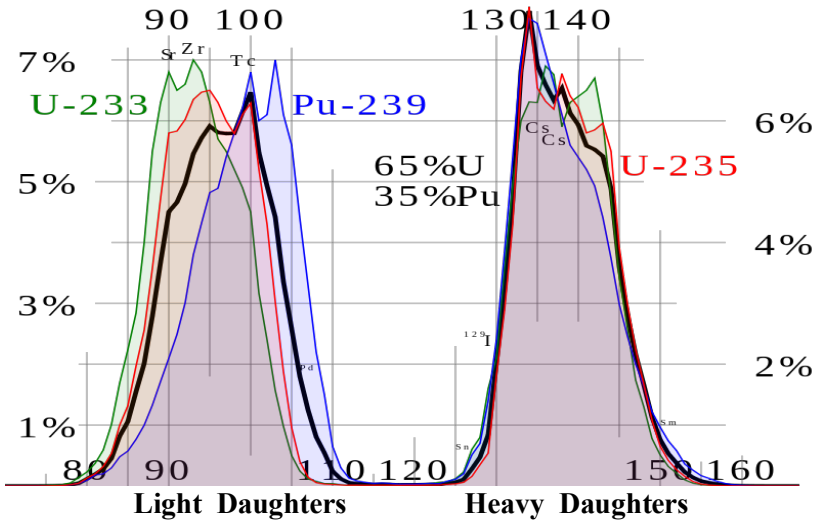

Figure 8.3 Bi-modal spectrum of fission products after early beta decays

Table 8.5 gives energy data of the most abundant initial two daughters before they undergo rapid beta$^-$ decay.

Nucleus	**$^{235}U \rightarrow$**	**n + ^{135}Te +**	**^{100}Zr**	**Energy Changes**
Energy	**A**	**B**	**C**	**ΔE = B + C - A**
Eb (MeV)	1783.0	1127	845.5	**ΔEb = 189.5** (MeV)
+ Ec (MeV)	909.0	344.6	225.1	**+ ΔEc = - 339.3**(MeV)
= En (MeV)	2692.0	1471.6	1070.6	**= ΔEn = -149.8**(MeV)
= En (NB)	556	304	221	**= ΔEn = - 31**(N B)

Table 8.5. Energy data for fission of ^{100}Zr from ^{134}Te..

A summary of similar data for some pairs of the initial daughters across the spectrum has enabled the formation of Fig. 8.6. Note that all initial daughters have $T_{1/2} < 3$ min. before beta$^-$ decay begins.

Mass No. A	**84**	**92**	**94**	**100**	**106**	**110**	**117**	**117**	**123**	**128**	**134**	**140**	**141**	**150**	**Bonds Broken**
Atomic No. Z	**34**	**36**	**38**	**40**	**42**	**44**	**46**	**46**	**48**	**50**	**52**	**54**	**56**	**58**	
Alpha No.	**17**	**18**	**19**	**20**	**21**	**22**	**23**	**23**	**24**	**25**	**26**	**27**	**28**	**29**	
Bonds	**186**	**201**	**210**	**223**	**236**	**246**	**261**	**261**	**275**	**290**	**303**	**306**	**325**	**340**	
7%				**Zr**							**Te**				**30**
6%			**Sr**									**Xe**			**30**
5%					**Mo**					**Sn**					**30**
4%		**Kr**											**Ba**		**30**
3%	**Se**													**Ce**	**30**
2%						**Ru**			**Cd**						**35**
1%							**Pd**	**Pd**							**34**

Light Daughters **Heavy Daughters**

Figure 8.4 Plot of data for fission model

Nuclear bond model of bi-modal spectrum of fission products of ^{235}U.

Fission occurs when the uranium nucleus is destabilized by absorbing a thermal neutron. The fusion energy released is sufficient to deform the liquid-like nucleus so that the asymmetric Coulomb field splits the nucleus. It is significant that all of these fissions break at least 30 (NB). Because layer 5 is attached to layer 4 by 60 bonds the bi-modal fission can be modelled as shown in Fig. 8.5.

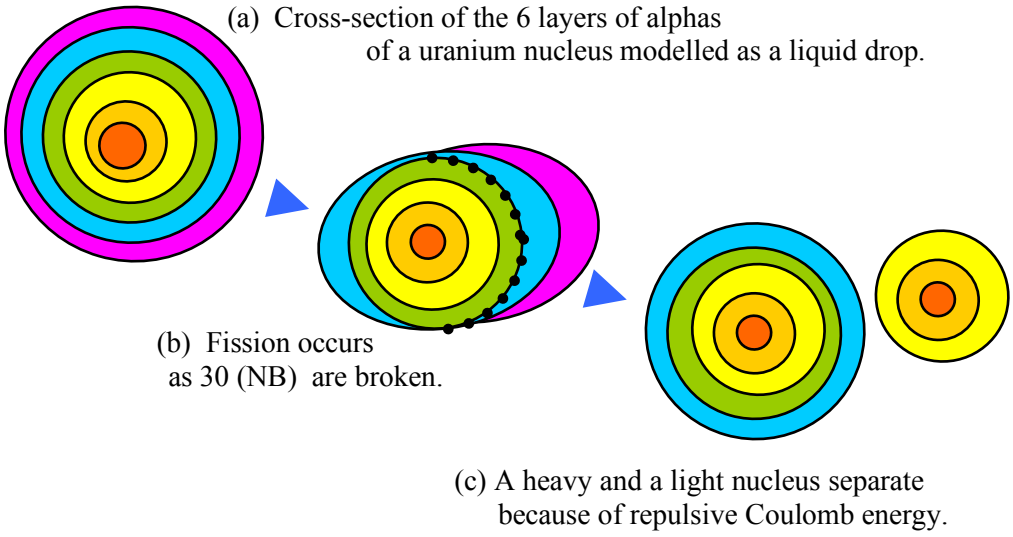

Figure 8.5. Schematic cross section model of uranium fission.

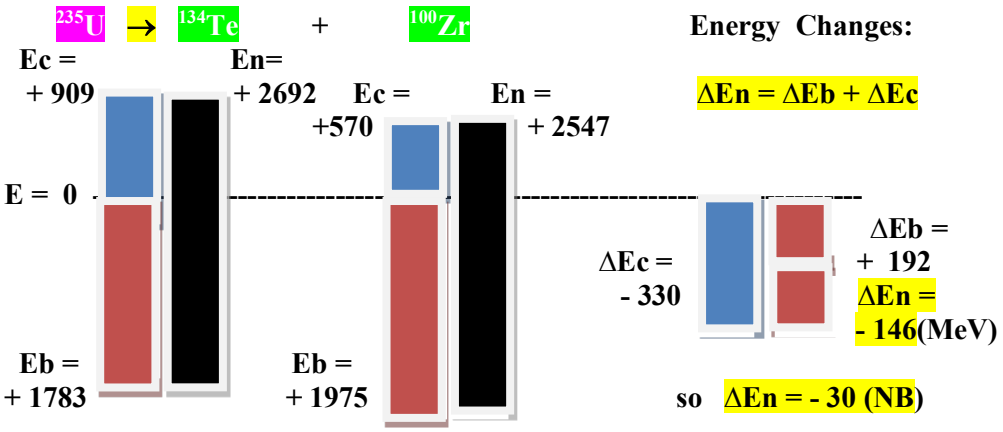

Figure 8.5 Energy changes during uranium fission.

Chapter 9. Nuclear Bond Structures

9.1 Nuclear Volume Packing Fractions.

The best measure of the packing of a nucleus is the volume packing fraction. As in metallurgy, this is simply the ratio of the total volume of the constituent spheres to the volume of their bounding space. In the case of the layered alpha model the volume packing fraction can be calculated as the ratio of the number of alphas times the volume of a single alpha divided by the volume of the nucleus concerned. For this purpose the volumes of some of those nuclei shown to be Fermi spheres, on the basis of their zero quadrupole moments, will be calculated using their outer charge density radii, R, as determined by Hofstadter et al [1963]. Because the fraction is between the volumes of spheres it reduces to a ratio of cubed radii as in Table 9.1.

Nucleus	R(fm)	$R^3(fm^3)$	Alphas.	Fraction
^{4}**He**	2.0	8.0	1	**1.0**
^{16}**O**	3.6	46.7	4	**0.69**
^{32}**S**	4.5	91.1	8	**0.70**
^{60}**Ni**	5.3	148.9	14	**0.75**
^{130}**Te**	6.6	287.5	26	**0.72**
^{190}**Os**	7.4	405.0	38	**0.75**

Table 9.1 Volume packing fractions of the 5 closed layer nuclei.

These approximate calculations show that the packing fraction is close to 0.74which is that of close-packed spheres in a face centred cubic lattice.

9.2 Nuclear tri-axial symmetry

In constructing densely packed alpha models of nuclei according to Bernal's models of liquid drops, it became apparent that the basic structure of ^{16}O, ^{32}S and ^{60}Ni is tetrahedral. The 3 orthogonal axes each pass through the mid points of opposing edges. However, in Figs. 9.2, 9.4 and 9.6, the vertical axis Z have been tilted back by 45^{o} and rotated clockwise by 45^{o} .

This monograph demonstrates that the structure of the nuclear bond models of heavier nuclei have the tri-axial symmetry of the next two Platonic solids, viz. the hexahedron and octahedron.

Each of the closed layer nuclei considered here is the most abundant isotope of its element which is more abundant than its neighbours.

The bond data shows that each alpha in the first layer is bound to its neighbours by 3 bonds and each alpha in the second layer is bound to the first layer by 3 bonds. Because of increased Coulomb repulsion, each alpha in layers three and four is bound to its inner layer by 4 bonds. For the same reason, each alpha in layers five and six is bound to its inner layer by 5 bonds.

As illustrated in Fig. 9.1, it is evident that the number of alphas in each layer of the models conforms with either the number of vertices, faces or edges of a tri-axial Platonic solid. It is also true that the number of extra neutrons increases until there is at least one added neutron for each alpha. In this way the nuclei are stabilised by additional nuclear binding energy.

Details of the triaxial symmetry of the 6 closed layer nuclei are displayed below.

The absense of alphas on the vertices of the octahedron prompted the proposition that they may be occupied by tritond in order to account for the stability and relative abundance of both ^{208}Pb and ^{251}Cf . Details of bond data and models conclude this account.

1. Tetrahedron

Alphas :	4	Vertices	4	Faces	6	Edges
Layer :	1		2		3	

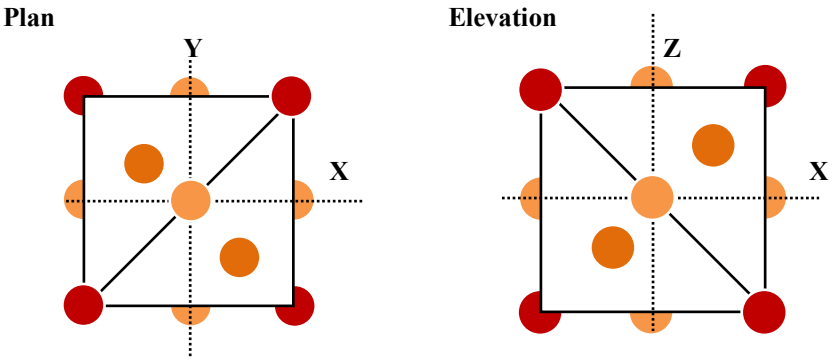

Figure 9.1 The tetrahedral structure of ^{4}H e, ^{16}O,^{32}S and ^{60}Ni.

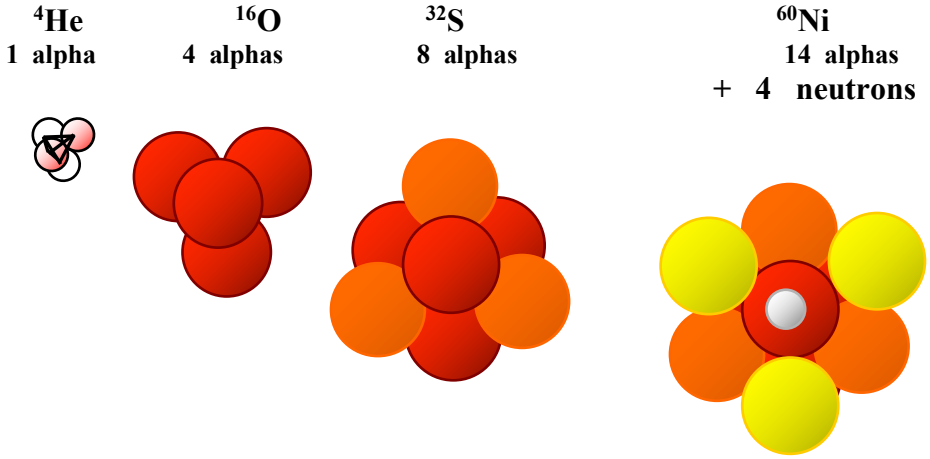

Figure 9.2 Models of ^{4}H e, ^{16}O,^{32}S and ^{60}Ni.

2. Hexahedron (Cube)

Alphas : (8 Vertices) (6 Faces) 12 Edges

Layer : 4

Plan or Elevation

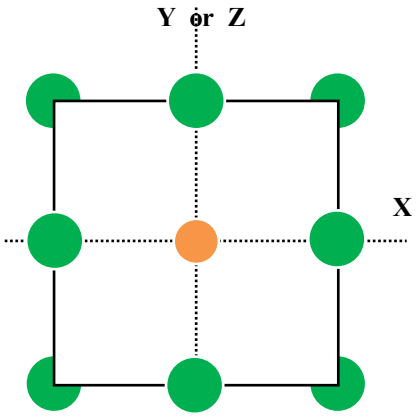

Figure 9.3 Hexahedral structure of ^{130}Te

^{130}Te 26 alphas + 26 neutrons

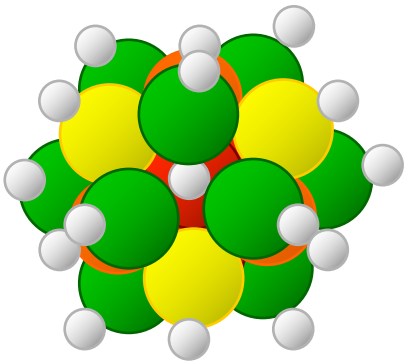

Figure 9.4 A model of ^{130}Te

3. Octahedron

Alphas : **(6 Vertices)** **8 Faces** **12 Edges**

Layer : **6** **5**

Plan or Elevation

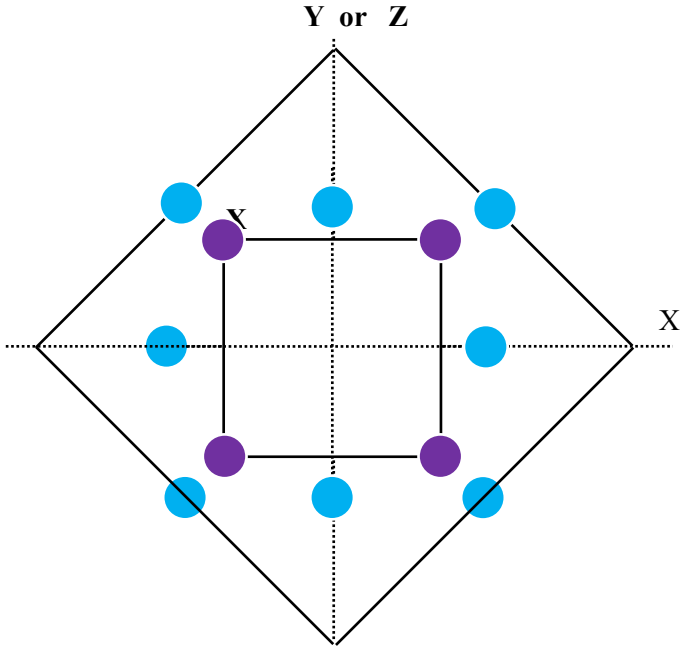

Figure 9.5 The octahedral structure of ^{190}Os and ^{238}U.

^{190}**Os**

38 alphas + 38 neutrons

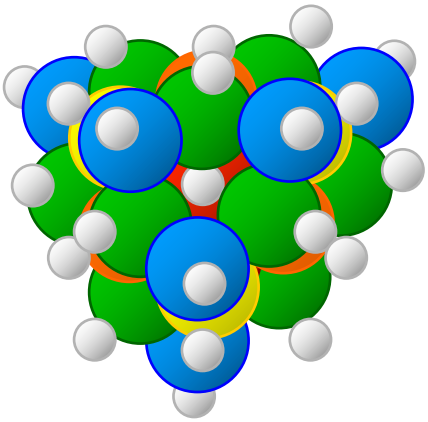

^{190}**Os**

^{238}**U**

46 alphas + 54 neutrons

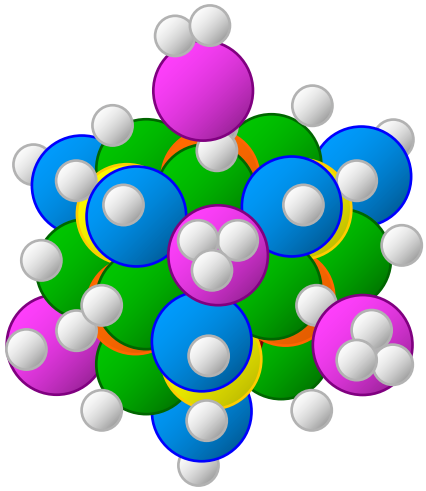

^{238}**U.**

Figure 9.6 Models of ^{190}Os and ^{238}U.

The absence of alphas from the 6 vertices of the octahedron pronpted the thought that perhaps the vertices may be occupied by tritons to account for the stability and relative abundance of both $^{208}Pb_{82}$ and $^{251}Cf_{98}$
The following nuclear bond data, models and figures appear to support this proposition.

Energy Nucleus	**Eb** (MeV)	**+ Ec** (MeV)	**= En** (MeV)	**= En (NB)**
$^{208}Pb_{82}$	1636	751	2387	493
$^{251}Cf_{98}$	1875	1011	2886	596

Table 9.2. Nuclear Bond data of ^{208}Pb and ^{251}Cf

Layers	**5**	**5+7**	**6**	**6+7**
Closed layer Nucleus	**^{190}Os**	**^{208}Pb**	**^{238}U**	**^{251}Cf**
Alphas in layer	12	12	8	8
(NB) in alphas	12x6=72	72	8x6=48	48
(NB) ex alphas	12x5=60	60	8x5=40	40
Tritrons in Layer 7	-	6	-	6
(NB) in Tritrons	-	6x1.8= 10.8	-	10.8
(NB) ex layer 7	-	6x4=24		24
(NB) in+ex layers	132	166.8	88	
(NB) in core	246+132 = 378	378+34.8 =412.8	378+88 = 466	466+ 34.8 =500.8
Neutrons in skin	38	38	54	55
(NB) ex skin	38x2 = 76	76	76+16x1 =92	93
Total (NB) in Model	454	489	558	594
Total (NB) from Data	450	493	559	596

Table 9.3 Nuclear Bond Models of ^{190}Os , ^{208}Pb, ^{238}U and ^{251}Cf

Octahedron ^{208}Pb

Alphas / Tritons: 6 Vertices (8 Faces) 12 Edges
Layer : 7 5
Plan or Elevation Y or Z

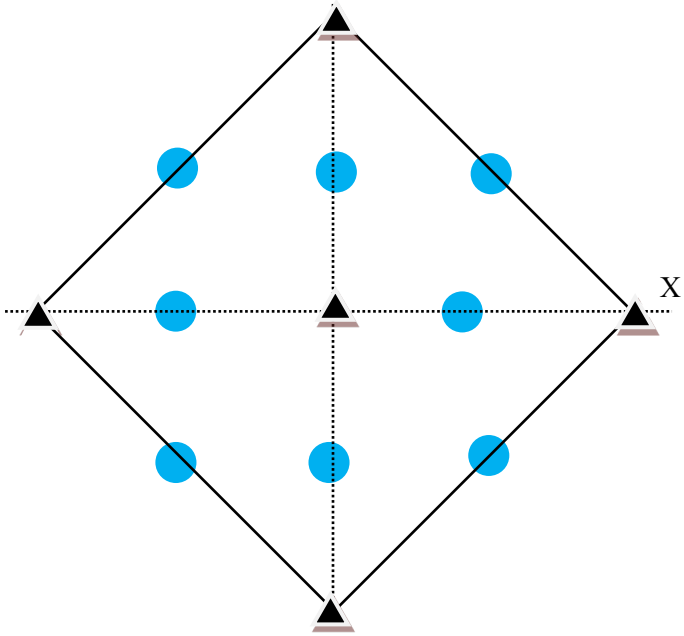

Figure 9.7 The octahedral structure of ^{208}Pb.

Octahedron ^{251}Cf

Alphas / Tritons:: 6 Vertices 8 Faces 12 Edges
Layer : 7 6 5
Plan or Elevation Y or Z

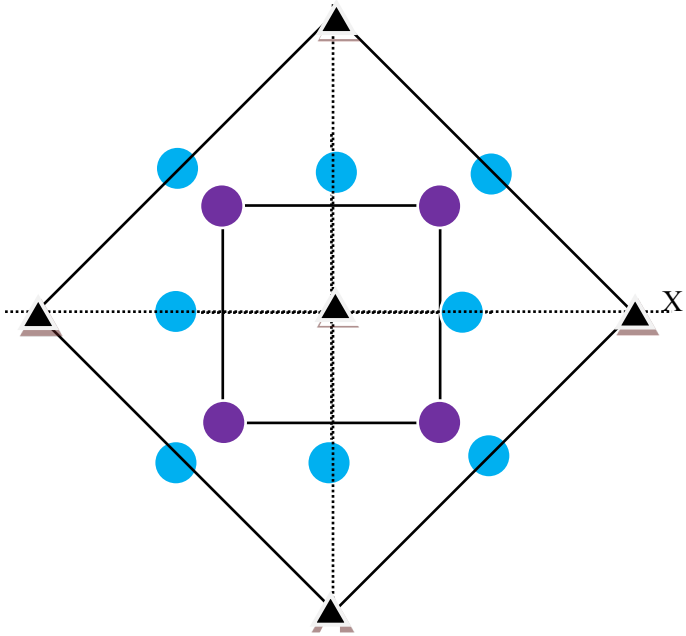

Figure 9.8 The octahedral structure of ^{251}Cf.

References:

Arnett,W.D. and Truran J.W.(1969) *Astrophys. J.*157,339.
Bailey,G., Griffith,G., Olivo,M. and Helmer,R. (1970) *Canad.J.Phys.* 483059.
Bargholtz, A.(1975) *Nucl.Phys.A*.243, 449.
Barnes,C. (1971). *Adv. Nuc.Phys.4.* 133.
Bernal,J.D. (1960) *Nature* 185,68.
Bethe,H. (1939) *Phys, Rev. 55* 193, 434.
Brink,D.M.(1966), Proc.Int.School of Physics Enrico Fermi, Course 36, Varenna,(1965), ed. C.Bloch (N.Y. Academic) 247.
Chaudhari,P.and Turnbull,D. (1978) *Science.*199, No.432,11.
de Takacsy,N. and das Gupta,S. (1970), *Phys.Lett.B* 33,556.
Dwarakanath,M. and Winkler,H. *(*1971) *Phys.Rev.C4*1532.
Dwarakanath,M. *(*1974) *Phys.Rev.C9*) 805.
Fowler,W. (1956) Sept.,Sci.Am.
Fowler,W. (1975) *Am.Rev/Astr.Ap.*1369.
Freidrich,H. Satpathy, L. and Weiguny,A.(1971) *Phys. Lett. B*. 36, 189.
Gontchar,I. Dasgupta,M., Hinde, D. Butt,R. and Mukherice,A. (2002) *Phys. Rev. C* 65 034610-1-8.
Griffith,G. Lal,M. and Scarfe, (1963) C., *Canad.J.Phys* 41. 724.
Hensley,D. (1967) *Ap.J.Phys.*147 818.
Hofstadter,R. (1963) "Nuclear and Nucleon Structure", W.A.Benjamin, New York.
Horiuchi,H., Ikeda,K. and Suzuki, Y. (1972) *Prog. Theor. Phtys. (Jap),* Suppl. 52, Chapt.3 .
Hoyle,F., Dunbar,D., Wenzel,W.. and Whaling,W. (1953) *Phys, Rev. 92.* 1095.
Hoyle,F.(1965)"Galaxies,Nuclei and Quasars", (Heinemann),London.147.
Ikeda,K., Takigawa, N. and Horiuchi,H., (1968) *Prog Theor. Phtys. (Jap),* Suppl. 464.
Kavanagh,R. in 'Essays in Nuclear Astro-physics' ed. C.Barnes, D.Clayton and D.Schramm (CU P1982)159
Kavanagh,R. (1960) *Nucl.,Phys 15* 411.
Kavanagh,R. (1969) *Bull.Am.Phys.Soc.14* 1209.
Lauritsen,C. quoted by W.Fowler, J.Greenstein and F.Hoyle (1961) in *Am.J.Phys.* 29393.
Norman,P. (1993) *Eur.J.Phys.* 14,36.
Norman,P. (2001) *Proc.Australian Nucl. Associationc.* 116.
Norman,P. (2003) *J.Phys. G: Nucl. Part Phys*. 29 B23-B28
Norman,P. (2006) *Proc A.I.P.17th Congress.82*
Norman,P. (2008) *Proc A.I.P.18th Congress.80*
Norman,P (2016) Australian Physics 53(2), 61-64
Ripka,G. (1967) "Fundamentals in Nuclear Theory", (Ed. by A.De-Shalt,C.Villi). (Int.Atomic
Rolfs, C. and Rodney, W. (1988). "Cauldrons in the Cosmos". U.C.P. Ch.8.
Sodenberg,A. (2008) *Nature*, 453, 469.
Thielemann, F.K. (1983) in "Cauldrons in the Cosmos" (by C.Rolfs & W.Rodney, U.C.P. 1986)
von Oertzen, W. (Hahn Meitner Inst. Berlin), Freer, M. (Birmingham Uni.) and Gridnev, K. (Uni. of St. Petersburg). (2004) Personal communications.